

220. 10/20/53  
111. 10/20/53

~~CONFIDENTIAL~~

Copy 241  
RM SL55L15

# NACA

## RESEARCH MEMORANDUM

for the

Bureau of Aeronautics, Department of the Navy

TANK TESTS OF A 1/8-SIZE POWERED DYNAMIC MODEL OF THE MARTIN  
PEM-5 SEAPLANE EQUIPPED WITH A SINGLE EDO HYDRO-SKI

TRD NO. NACA AD3110

By Claude W. Coffee, Jr.

Langley Aeronautical Laboratory  
Langley Field, Va.

CLASSIFICATION CHANGED

UNCLASSIFIED

To \_\_\_\_\_

*John B. ...*

By authority of *John B. ...* Date *10/20/53*  
CLASSIFIED DOCUMENT

This document contains classified information affecting the National Defense of the United States within the meaning of the Espionage Act, USC 182703 and 794. Its transmission or the revelation of its contents in any manner to an unauthorized person is prohibited by law.

NATIONAL ADVISORY COMMITTEE  
FOR AERONAUTICS  
WASHINGTON

~~CONFIDENTIAL~~



NATIONAL ADVISORY COMMITTEE FOR AERONAUTICS

RESEARCH MEMORANDUM

for the

Bureau of Aeronautics, Department of the Navy

TANK TESTS OF A 1/8-SIZE POWERED DYNAMIC MODEL OF THE MARTIN  
PBM-5 SEAPLANE EQUIPPED WITH A SINGLE EDO HYDRO-SKI

TED NO. NACA AD3110

By Claude W. Coffee, Jr.

SUMMARY

An investigation was made of the hydrodynamic characteristics of a 1/8-size powered dynamic model of the Martin PBM-5 seaplane equipped with a single Edo hydro-ski. The hydro-ski was similar in shape to that used during model and full-scale tests of the Grumman JRF-5 airplane. Various hydro-ski positions were investigated.

The excess thrust available at hump speeds decreased as the strut length increased. Landing stability in smooth water was satisfactory. In smooth water, stable take-offs could be made except in the aft position and when the hydro-ski had 2° incidence.

INTRODUCTION

Interest has been shown recently in modifying the Martin PBM-5 patrol bomber for use as an ASW sonar seaplane. The modification includes the use of an Edo Corporation hydro-ski to improve the rough-water capabilities of the airplane. The Edo hydro-ski is similar to that used on the Grumman JRF-5 airplane (ref. 1) but is retractable.

In order to determine the hydrodynamic adequacy of the proposed modification, the Bureau of Aeronautics, Department of the Navy, requested that an abbreviated tank evaluation be made using an existing 1/8-size powered dynamic model of the PBM-5 seaplane. The resistance, take-off

and landing stability, and spray characteristics were determined for several positions of the hydro-ski. Visual observations were made and motion pictures were taken of the behavior in rough water.

### SYMBOLS

$\delta_e$	elevator deflection referred to stabilizer chord, positive when trailing edge is down, deg
$\delta_f$	flap deflection referred to wing chord, positive when trailing edge is down, deg
$r$	rise of center of gravity, assumed to be positive in an upward direction and to be zero when hull step touched undisturbed water at a trim angle of $0^\circ$ , ft
$\tau$	trim assumed to be the angle between horizontal and forebody keel at step, deg

### DESCRIPTION OF MODEL

Photographs and a general-arrangement drawing of the model are shown in figures 1 and 2. Pertinent characteristics and dimensions of the model and full-size seaplane are given in table I. Photographs and general arrangement of the hydro-ski are shown in figures 3 and 4. Offsets of the hydro-ski are given in table II. The hydro-ski strut ordinates are given in table III.

Conventional balsa construction was used for the model and aerodynamic surfaces. Leading-edge slats were attached to the wing in order to delay the stall to an angle of attack more nearly equal to that at which the full-size seaplane would stall. The flaps were of the single-slotted type extending over approximately 65 percent of the wing span.

The hydro-ski and hydro-ski strut were made of mahogany. The five positions of the hydro-ski tested are as shown in the following table:

Configuration	Vertical distance from hull keel to hydro-ski keel at trailing edge, ft	Horizontal distance from hull step to hydro-ski trailing edge (positive forward), ft	Angle between hull keel at step and hydro-ski keel, deg
Long strut	6.00	0.04	0
Intermediate strut	3.33	0.04	0
Short strut	1.50	0.04	0
Aft ski (long strut)	6.00	-1.96	0
2° incidence (long strut)	6.00	0.04	2

The dynamic model was powered by two 5-horsepower 3-phase alternating-current induction motors. Because of excessive damage caused by hull spray, the wooden propellers with which the tests were begun were replaced by metal propellers.

#### APPARATUS

A description of Langley tank no. 1 and the towing carriage is given in reference 2. The model was pivoted at the center of gravity and had freedom only in rise and trim except for landings in smooth and rough water and take-offs in rough water, during which approximately 5 feet of fore-and-aft freedom with respect to the towing carriage was provided. Slide-wire pickups were used to measure trim, rise, and fore-and-aft position of the model.

Aerodynamic lift and moment were measured with spring dynamometers. Horizontal force was measured by the resistance dynamometer described in reference 2.

Regular trains of transverse waves were generated by the tank no. 1 wave maker for the rough-water tests.

### Aerodynamic Qualities

Effective thrust.- The effective thrust of the model (defined as the difference in the resultant horizontal force power-on and power-off) was determined at 0° trim, 30° flap deflection, 0° elevator deflection, with the step of the model approximately 9 inches (model size) above the water surface.

Aerodynamic lift and pitching moment.- The aerodynamic lift and pitching moment, without power, for various flap and elevator deflections and various trims were measured with the model supported in the air in the same position as that used for the determination of the thrust. The center of moments was located at a center-of-gravity position corresponding to 25 percent mean aerodynamic chord ( $\bar{c}$ ).

### Hydrodynamic Qualities

The determination of the hydrodynamic qualities was made at a gross load corresponding to 51,000 pounds full-size, with the flaps deflected 30°. The center of gravity for all tests was located at 0.25 $\bar{c}$ .

Excess thrust.- The excess thrust, which is the force available for acceleration during take-off, is defined as the difference between the effective thrust and the resultant horizontal force, power-on, for the complete model. The excess thrust was measured for various fixed-elevator deflections over a range of speeds and the maximum excess thrust was determined from cross plots. The corresponding trim and rise were recorded.

Landing stability.- With the model flying at the desired landing trim, the towing carriage was decelerated at a uniform rate so that the model was allowed to glide onto the water in simulation of an actual landing. The model was held in trim by a trim brake which was released electrically upon contact with the water. The landings were made without power and the elevators were set so that the aerodynamic pitching moment about the center of gravity would be approximately zero at the instant of contact. The deceleration of the towing carriage was adjusted so that the fore-and-aft travel of the model was kept within the limits of the gear. Time-history recordings were made of the trim, rise, fore-and-aft position, and speed. Visual observations and motion pictures also were made.

Take-offs in smooth and rough water.- Runs were made to take-off speed at a constant rate of acceleration of 1 foot per second per second with a range of fixed elevators. Trim, rise, and speed were recorded continuously during the accelerated runs. Motion pictures were also made during these runs.

Spray characteristics.- Spray observations and photographs with the accompanying values of trim and rise were made for a range of constant-speed runs.

RESULTS AND DISCUSSION

All model quantities have been converted to full-size values except where otherwise noted.

Aerodynamic

The effective model thrust converted to full-size values is plotted against speed in figure 5. The effective thrust approximates the estimated thrust (ref. 3) throughout the speed range investigated.

The aerodynamic lift and pitching-moment coefficients, at a speed of 67 knots, for the power-off condition are plotted against trim in figure 6 for two flap and elevator deflections. All subsequent tests were made with 30° flap deflection. It should be pointed out that the results include the ground effect due to the proximity of the water.

Hydrodynamic

In order to permit a more detailed study of the results obtained for any of the configurations tested, the basic data are plotted in the following figures:

	Figure
Basic hull:	
Excess thrust . . . . .	7
Spray photographs . . . . .	8
Long-strut configuration:	
Excess thrust . . . . .	9
Smooth-water landing characteristics . . . . .	10
Smooth-water take-off characteristics . . . . .	11
Rough-water take-off behavior:	
Envelopes of trim and rise in waves	
6 feet high and 288 feet long . . . . .	12
Effect of elevator deflection in	
waves 6 feet high and 288 feet long . . . . .	13
Effect of wave height and length . . . . .	14
Spray photographs . . . . .	15

	Figure
Intermediate-strut configuration:	
Excess thrust . . . . .	16
Smooth-water take-off characteristics . . . . .	17
Rough-water take-off behavior:	
Effect of wave height and length . . . . .	18
Spray photographs . . . . .	19
Short-strut configuration:	
Excess thrust . . . . .	20
Smooth-water landing characteristics . . . . .	21
Smooth-water take-off characteristics . . . . .	22
Rough-water take-off behavior:	
Effect of wave height and length . . . . .	23
Spray photographs . . . . .	24
Aft-ski configuration:	
Excess thrust . . . . .	25
Smooth-water landing characteristics . . . . .	26
Smooth-water take-off characteristics . . . . .	27
Rough-water take-off behavior:	
Envelopes of trim and rise in waves	
6 feet high and 288 feet long . . . . .	28
Effect of elevator deflection . . . . .	29
Effect of wave height and length . . . . .	30
2°-incidence, long-strut configuration:	
Excess thrust . . . . .	31
Smooth-water take-off characteristics . . . . .	32

The discussion of the results obtained during the tests is confined mainly to comparison and to visual observations that are not apparent from the figures.

Excess thrust.- The excess thrust available at hump speeds, where excess thrust is normally a minimum, was 7,600 pounds (fig. 7) for the basic hull. This excess thrust was reduced by extending the hydro-ski, as the comparison in figure 33 indicates. An increase in vertical distance of the hydro-ski below the hull from 1.5 feet to 6 feet decreased the excess thrust from 5,100 pounds to 2,900 pounds. This decrease in excess thrust (increased resistance) may be partially attributed to the higher emergence trims of the longer-strut configurations.

The minimum excess thrust occurred at a speed of approximately 30 knots as the hydro-ski emerged. Emergence was stable for the basic hydro-ski configuration (trailing edge of hydro-ski, 0.04 foot forward of the step; incidence, 0°).

With the hydro-ski in the aft position, the excess thrust at the hump was increased from 2,900 pounds (fig. 9) to 4,500 pounds (fig. 25) but lower-limit porpoising occurred after emergence. There was no range of stable trim from 34 to 42 knots with the available aerodynamic trimming moments.

An increase in hydro-ski incidence of  $2^\circ$  increased the available excess thrust at the hump from 2,900 pounds (fig. 9) to 3,800 pounds with an elevator deflection of  $-7\frac{1}{2}^\circ$  (fig. 31). The emergence, however, was unstable.

Smooth-water landings.- The maximum and minimum values of the trim and rise at the greatest cycle of oscillation during the landing run are compared in figure 34. These changes in trim and rise are those that occurred during the high-speed portion of the landing runout, before hydro-ski submergence. The oscillations appeared to be the result of the configurations seeking an equilibrium condition rather than a porpoising cycle. The long-strut configuration gave smaller amplitudes of both trim and rise oscillation over the range of landing trims investigated. In general, the landing stability was satisfactory.

Smooth-water take-offs.- The emergence instability that has been noted during tests of other hydro-ski configurations (ref. 1) was apparent during these tests with only the configuration having  $2^\circ$  incidence (fig. 32). This instability occurred over a speed range from 27 to 32 knots. Emergence was stable for all other configurations. After emergence there was a tendency for the model to oscillate for several cycles before reaching an equilibrium condition. No upper-limit porpoising was encountered during take-offs with any of the hydro-ski configurations. Lower-limit porpoising, however, appeared to limit the range of elevator deflection that might be used for take-offs.

The maximum amplitudes of porpoising are plotted against elevator deflection in figure 35 for the three strut lengths. Assuming a maximum allowable amplitude of porpoising of  $2^\circ$  for satisfactory take-off, the strut length had no appreciable effect on the minimum elevator deflection that might be used; however, the increase of porpoising amplitude with elevator deflection once instability is encountered is appreciably less with the long-strut configuration.

The maximum amplitude of porpoising for the two hydro-ski incidences is plotted against elevator deflection in figure 36. The increase in incidence of the hydro-ski permitted a lower elevator deflection to be used before lower-limit porpoising was encountered, as would be expected from the increased trim of the planing surface involved.

The effect of longitudinal hydro-ski position on the trim and rise during take-offs in smooth water is shown in figure 37. With the hydro-ski in the aft position, the trims were decreased throughout the take-off and the model trimmed into lower limit with full-up elevators ( $-20^\circ$ ), so that no stable take-off could be made.

Rough-water take-offs.- At low speeds during rough-water take-offs, the model tended to follow the waves, and the changes in trim and rise were approximately the same as the changes in wave slope and height, respectively. Consequently, the motions in the shorter and steeper waves were more violent. At high speeds after emergence, the motions were more violent for the higher waves and did not show a consistent trend with changes in wave length. This inconsistency was due to the fact that in some instances the hydro-ski would skip from crest to crest, giving small changes in trim and rise, and in others the hydro-ski would follow the wave slope, resulting in large changes in trim and rise (figs. 14, 18, 23, and 30). The reduction in motions which might be anticipated from increasing the strut length was not apparent in the data. Such a result might be expected if the size of the ski were too large to allow penetration to the extent that the hull contacts the water.

A comparison of the envelopes of the trim and rise obtained during a series of take-offs in one wave condition is presented in figure 38 for the two longitudinal hydro-ski positions. This figure indicates a slight decrease in the maximum amplitudes with the hydro-ski in the aft position; however, as previously pointed out, smooth-water take-off stability was unacceptable with this configuration.

Spray.- Heavy bow spray struck the propellers of the basic model in the pre-emergence speed range from 13 to 20 knots. There appeared to be no effect of the hydro-ski on this bow spray. Damage to the wooden propellers by this bow spray necessitated a change to metal propellers early in the tests. Light spray entered the propellers briefly during emergence for all hydro-ski configurations. Spray on the tail surfaces at high speeds was heavier for the hydro-ski configurations than for the basic hull.

## CONCLUSIONS

The results of the hydrodynamic investigation of a 1/8-size model of the Martin PBM-5 equipped with a single hydro-ski indicated that:

1. The excess thrust at the hump speeds decreased as the strut length increased and increased with either aft movement of the hydro-ski or increase in hydro-ski incidence.

2. The landing characteristics in smooth water were satisfactory.
3. Stable take-offs in smooth water could be made except in the aft position and when the hydro-ski had 2° incidence.
4. The maximum changes in trim and rise during take-offs in waves appeared to decrease as the hydro-ski position was moved aft.
5. Light spray struck the propellers briefly during hydro-ski emergence and there appeared to be no effect of the hydro-ski on the heavy bow spray prior to emergence.

Langley Aeronautical Laboratory,  
National Advisory Committee for Aeronautics,  
Langley Field, Va., November 29, 1955.

*Claude W. Coffee Jr.*  
Claude W. Coffee, Jr.  
Aeronautical Research Scientist

Approved:

*John B. Parkinson*  
John B. Parkinson  
Chief of Hydrodynamics Division

gfw

#### REFERENCES

1. Wadlin, Kenneth L., and Ramsen, John A.: Tank Investigation of the Grumman JRF-5 Airplane Fitted With Hydro-Skis Suitable for Operation on Water, Snow, and Ice. NACA RM L9K29, 1950.
2. Truscott, Starr: The Enlarged NACA Tank, and Some of Its Work. NACA TM 918, 1939.
3. Anon.: Proposal for Anti-Submarine Warfare Airplane. Rep. 3828, Edo Corp. (College Point, N. Y.), Jan. 8, 1954.

TABLE I.- PERTINENT CHARACTERISTICS AND DIMENSIONS  
OF MODEL AND FULL-SIZE SEAPLANE

	Model size	Full size
<b>General:</b>		
Gross load, lb . . . . .	898.5	51,000
Wing area, sq ft . . . . .	22	1,408
Overall length, ft . . . . .	10	80
<b>Hull:</b>		
Length of forebody, ft . . . . .	4.2	33.5
Length of afterbody, ft . . . . .	3.4	27.4
Length of tail cone, ft . . . . .	2.4	19.1
Beam at chine at step, ft . . . . .	1.25	10
Forebody-length—beam ratio . . . . .	3.4	3.4
Afterbody-length—beam ratio . . . . .	2.7	2.7
Overall-length—beam ratio . . . . .	6.1	6.1
<b>Step:</b>		
Type . . . . .	Transverse	Transverse
Depth at keel, in. . . . .	0.73	5.8
Forebody dead rise at step, deg . . . . .	20	20
<b>Hydro-ski:</b>		
Length, ft . . . . .	2.03	16.2
Beam, ft . . . . .	0.585	4.68
Length-beam ratio . . . . .	3.47	3.47
Area, sq ft . . . . .	8.25	66
<b>Hydro-ski strut:</b>		
Chord, in. . . . .	4.5	36
Maximum thickness, in. . . . .	1.25	10
Airfoil section . . . . .	NACA 16-027.8 (modified)	NACA 16-027.8 (modified)
<b>Wing:</b>		
Area, sq ft . . . . .	22	1408
Span, ft . . . . .	14.8	118
Root chord, ft . . . . .	2.3	18
Tip chord, ft . . . . .	0.75	6
Mean aerodynamic chord, ft . . . . .	1.6	13
Aspect ratio . . . . .	9.9	9.9
Taper ratio . . . . .	3.1	3.1
Angle of incidence, deg . . . . .	3	3
<b>Flap:</b>		
Type . . . . .	Slotted	Slotted
Total area, sq ft . . . . .	3.2	204
Chord, ft . . . . .	0.4	3.4
<b>Section:</b>		
Root . . . . .	NACA 23020	NACA 23020
Tip . . . . .	NACA 23010 (modified)	NACA 23010 (modified)
<b>Horizontal tail:</b>		
Area, projected plane, sq ft . . . . .	3.7	234
Span, projected plane, ft . . . . .	3.4	27.2
Chord, ft . . . . .	1.16	9.3
Dihedral . . . . .	15	15
Aspect ratio, projected plane . . . . .	3.16	3.16
Section . . . . .	NACA 0012-64	NACA 0012-64
<b>Elevators:</b>		
Total area, sq ft . . . . .	1.2	96
<b>Movement:</b>		
Up, deg . . . . .	25	25
Down, deg . . . . .	5	20
<b>Vertical tail (two):</b>		
Total area, projected plane, sq ft . . . . .	2.33	186
Span, projected plane, ft . . . . .	1.7	13.9
Aspect ratio, projected plane . . . . .	2.08	1
Section . . . . .	NACA 0009-64	NACA 0009-64

<sup>a</sup>Specific weight of water in Langley tank no. 1 for these tests was 63.3 lb/cu ft as compared with 64.0 lb/cu ft for sea water.

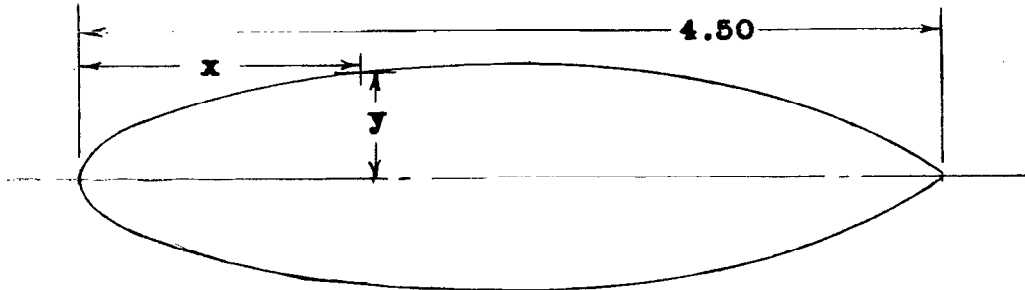
TABLE II.- OFFSETS OF HYDRO-SKI FOR LANGLEY TANK NO. 1 MODEL 210

[All dimensions are in inches, model size]

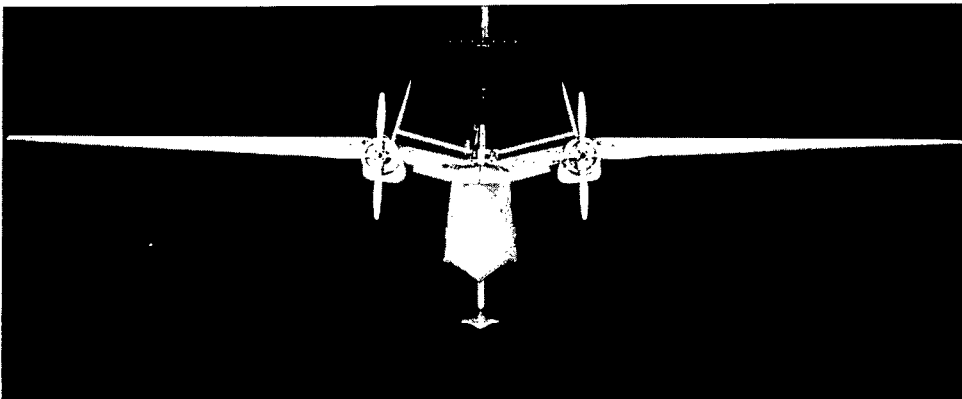
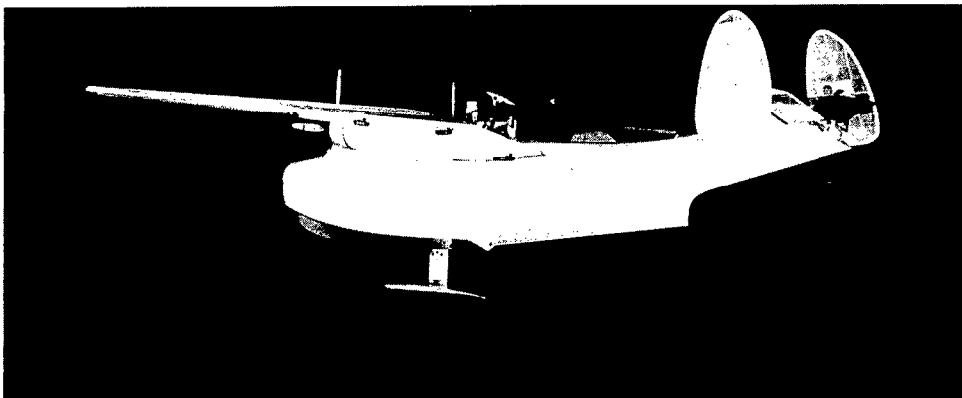
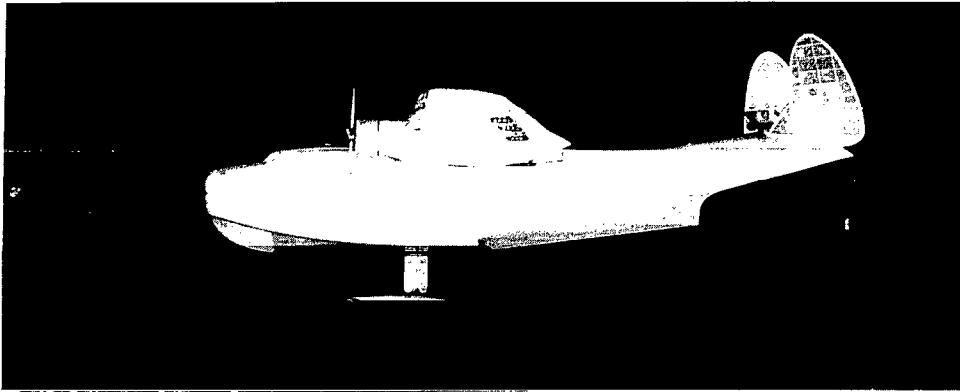
Station	Distance to sta. 0	Keel above B.L.	Chine above B.L.	Half-beam at chine	Height of hydro-ski at $\xi$	Buttock lines													
						0.23	0.47	0.70	0.94	1.17	1.40	1.87	2.34	2.80	3.27				
0	0	1.34	1.34	0	1.34														
1	.47	.73	1.37	1.09	1.48	1.48	1.48	1.48	1.26	1.34									
2	.94	.43	1.36	1.54	1.58	1.58	1.58	1.58	1.06	1.22	1.57	1.49							
3	1.40	.26	1.32	1.91	1.68	1.68	1.68	1.68	1.04	1.68	1.65	1.38							
4	2.34	.11	1.23	2.50	1.81	1.81	1.81	1.81	.69	1.81	1.80	1.72	1.48						
5	3.04	.06	1.16	2.86	1.89	1.89	1.89	1.89	.47	1.89	1.88	1.82	1.69	1.29					
6	3.97	.03	1.08	3.23	1.97	1.97	1.97	1.97	.31	1.97	1.96	1.91	1.82	1.61					
7	5.61	0	1.01	3.51	2.08	2.08	2.08	2.08	.22	2.08	2.07	2.03	1.95	1.79	1.46				
8	8.76	0	1.01	3.51	2.16	2.16	2.16	2.16	.22	2.16	2.15	2.11	2.04	1.87	1.52				
9	11.57	0	1.01	3.51	2.11	2.11	2.11	2.11	.22	2.11	2.10	2.06	1.99	1.85	1.52				
10	14.37	0	1.01	3.51	1.97	1.97	1.97	1.97	.22	1.97	1.96	1.94	1.87	1.74	1.47				
11	16.83	0	1.01	3.51	1.76	1.76	1.76	1.76	.22	1.76	1.76	1.74	1.69	1.58	1.34				
12	19.17	0	.99	3.21	1.49	1.49	1.49	1.49	.22	1.49	1.49	1.47	1.42	1.31					
13	21.50	0	.85	2.45	1.12	1.12	1.12	1.12	.22	1.12	1.12	1.07	.93						
14	22.90	0	.68	1.90	.84	.84	.84	.84	.22	.84	.84	.82	.70						
15	24.31	0	.42	1.29	.51	.51	.51	.51	.22	.47									

TABLE III.- STRUT OFFSETS

[All dimensions are in inches, model size]



Offsets	
Station, $x$	Half breadth, $y$
0	0
.06	.13
.11	.19
.22	.26
.34	.32
.45	.36
.68	.43
.90	.49
1.35	.56
1.80	.61
2.25	.625.
2.70	.61
3.15	.55
3.60	.44
4.05	.26
4.28	.15
4.50	.01
L.E. radius = 0.13	



L-91703

Figure 1.- Photographs of 1/8-size model of Martin PBM-5 seaplane equipped with a single hydro-ski.

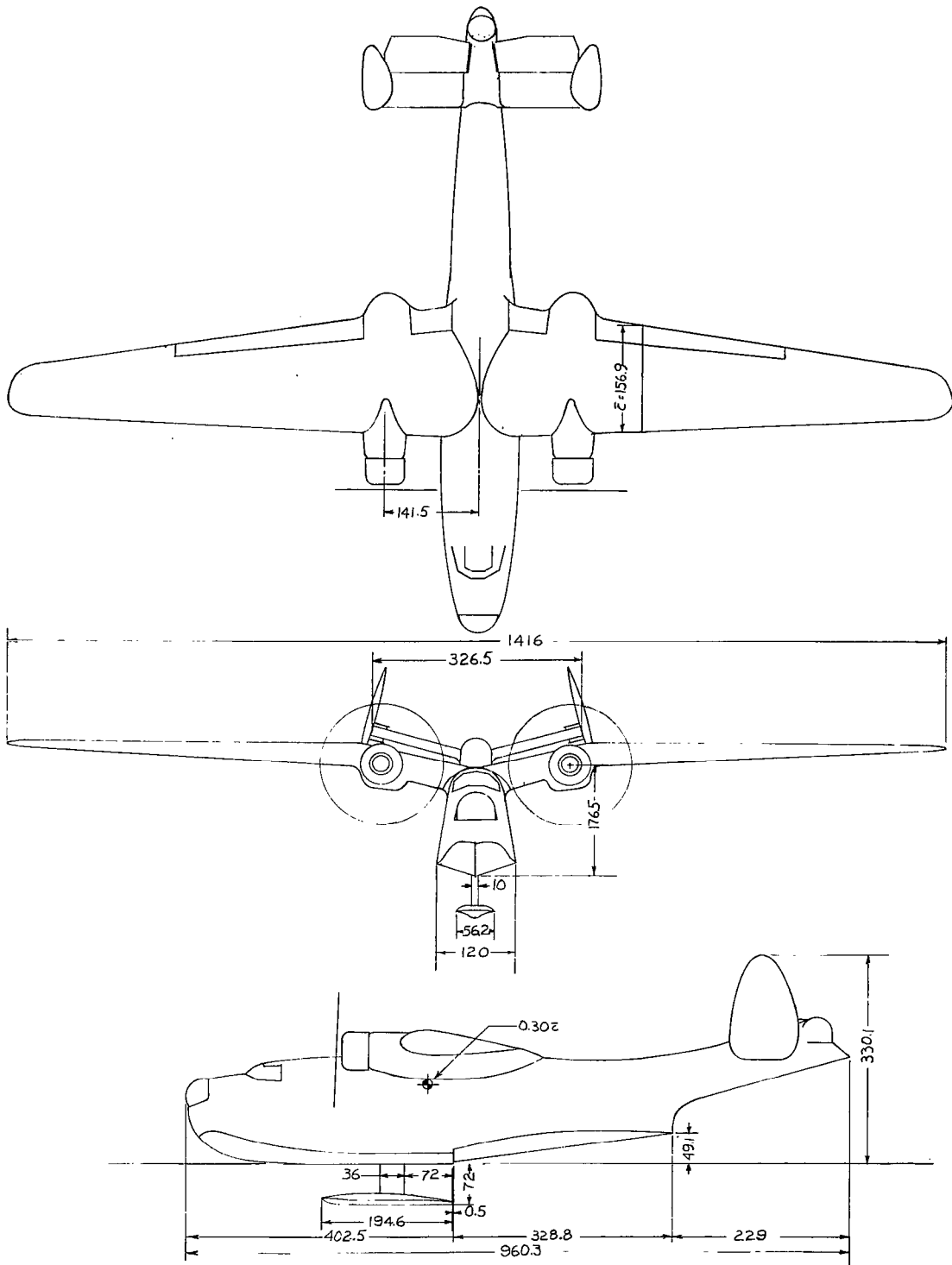
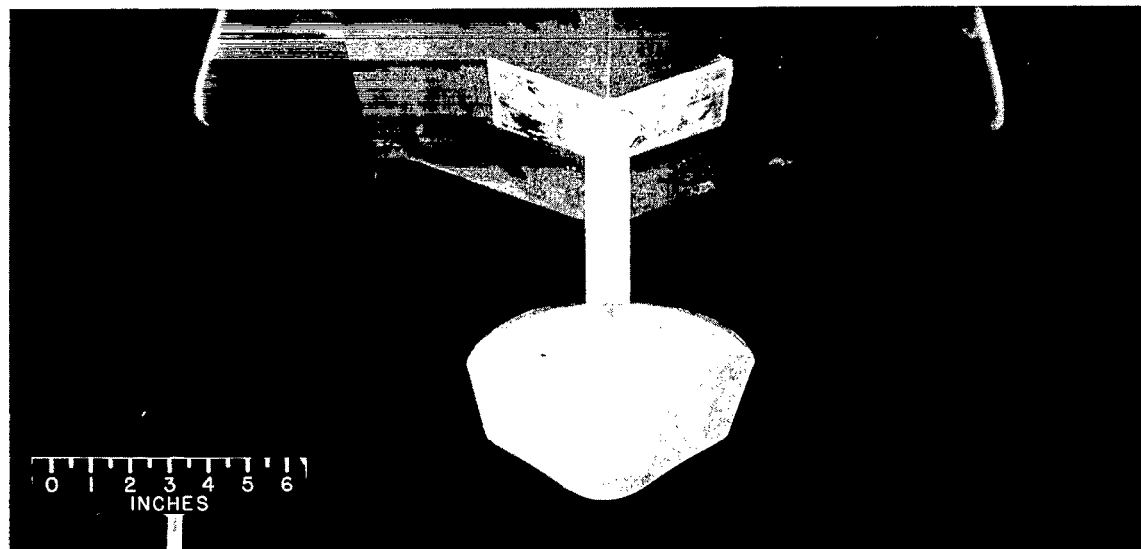
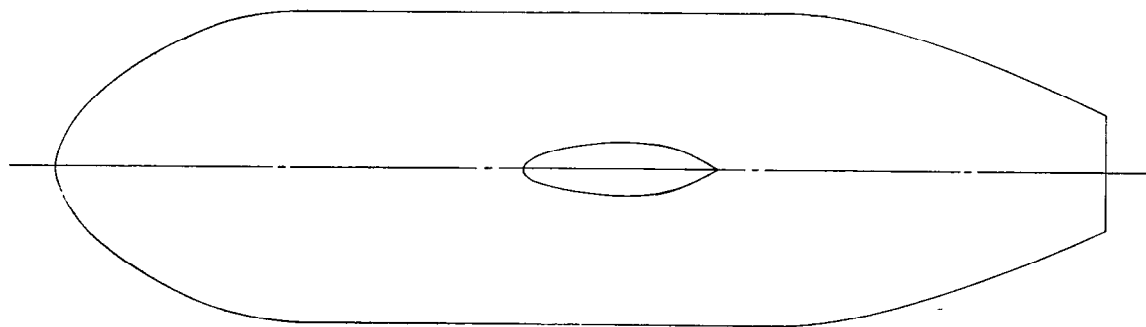


Figure 2.- General arrangement of Martin PBM-5 seaplane equipped with a single hydro-ski. (All dimensions are in inches, full size.)



L-91704

Figure 3.- Photographs of hydro-ski for Martin PBM-5 seaplane.



	STRUT LENGTH
Short strut	18
Intermediate strut	40
Long strut	72

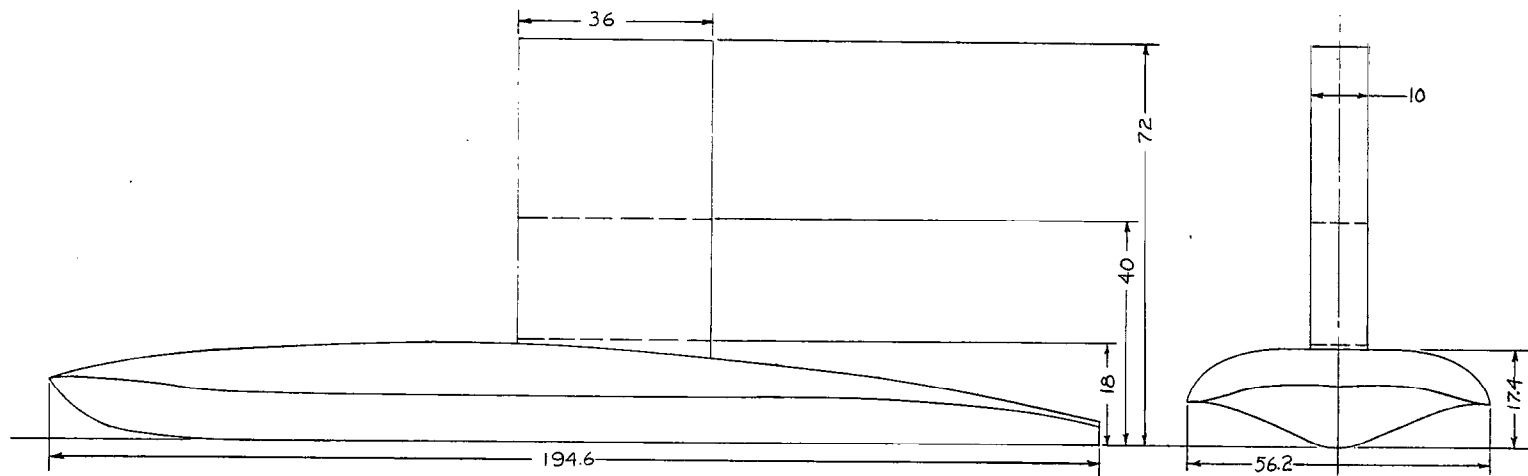


Figure 4.- General-arrangement drawing of hydro-ski. (All dimensions are in inches, full size.)

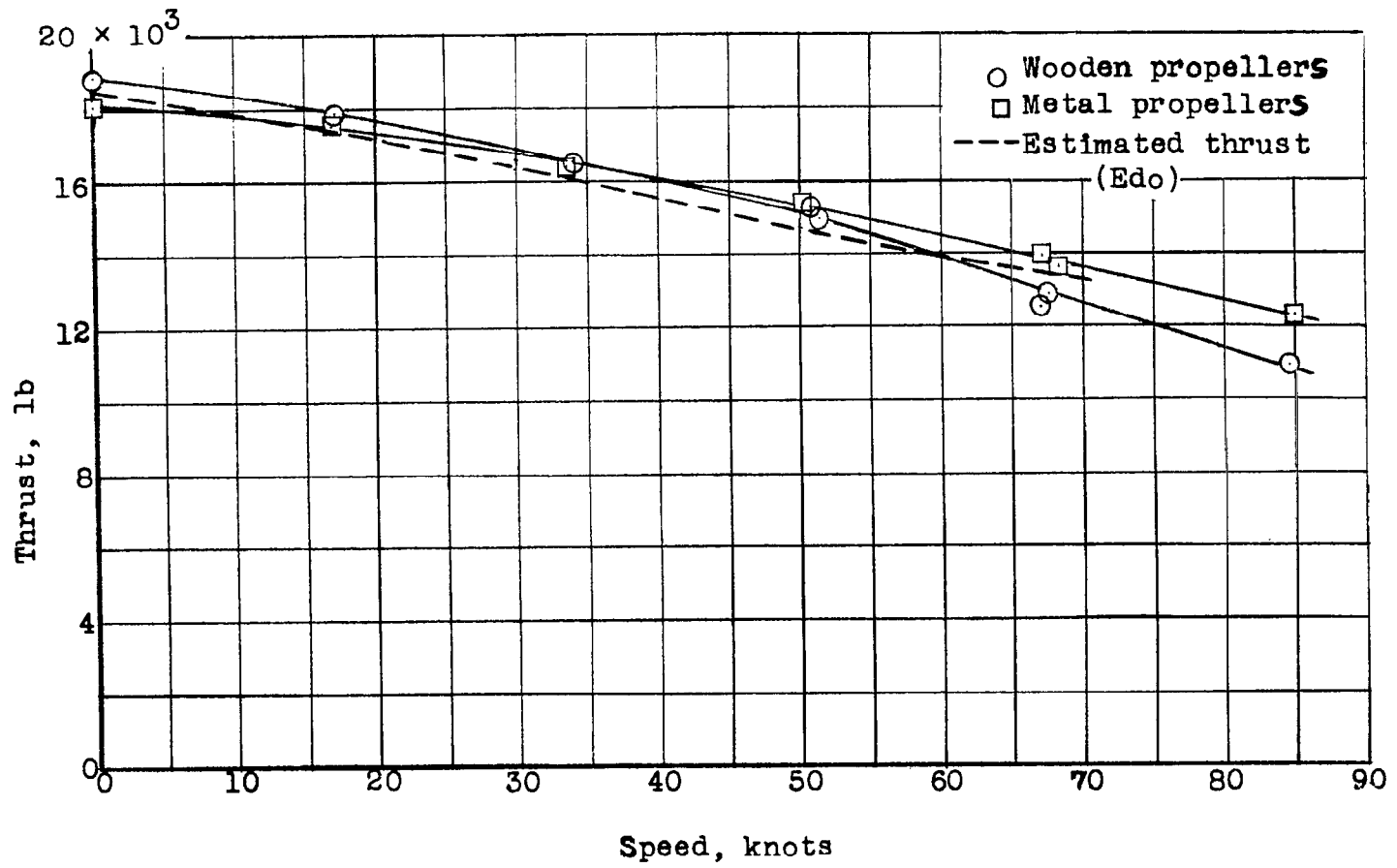


Figure 5.- Effective thrust.  $\tau = 0^\circ$ ;  $\delta_f = 30^\circ$ ;  $\delta_e = 0^\circ$ .

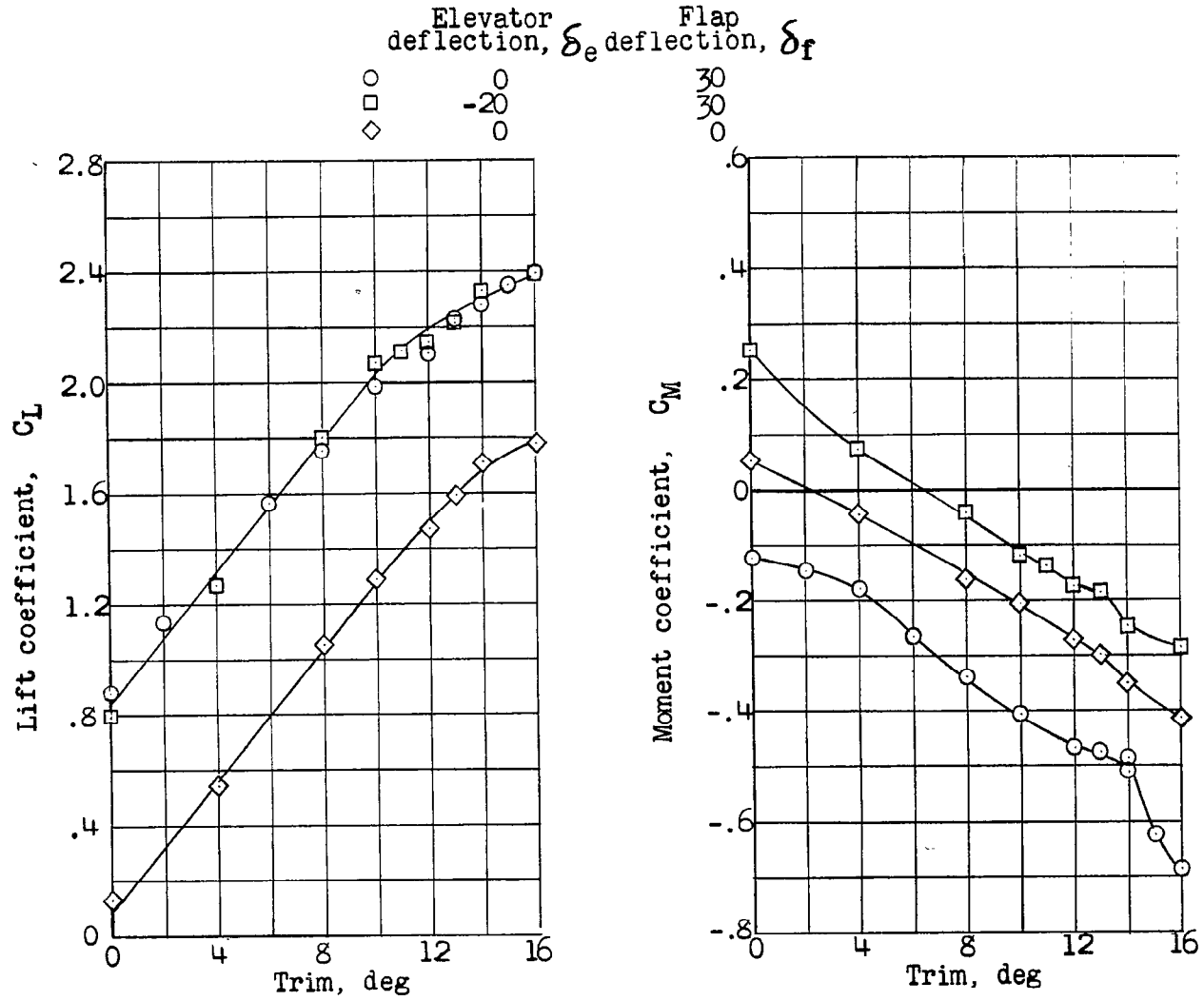


Figure 6.- Variation of aerodynamic lift and pitching-moment coefficients with trim. Power-off.

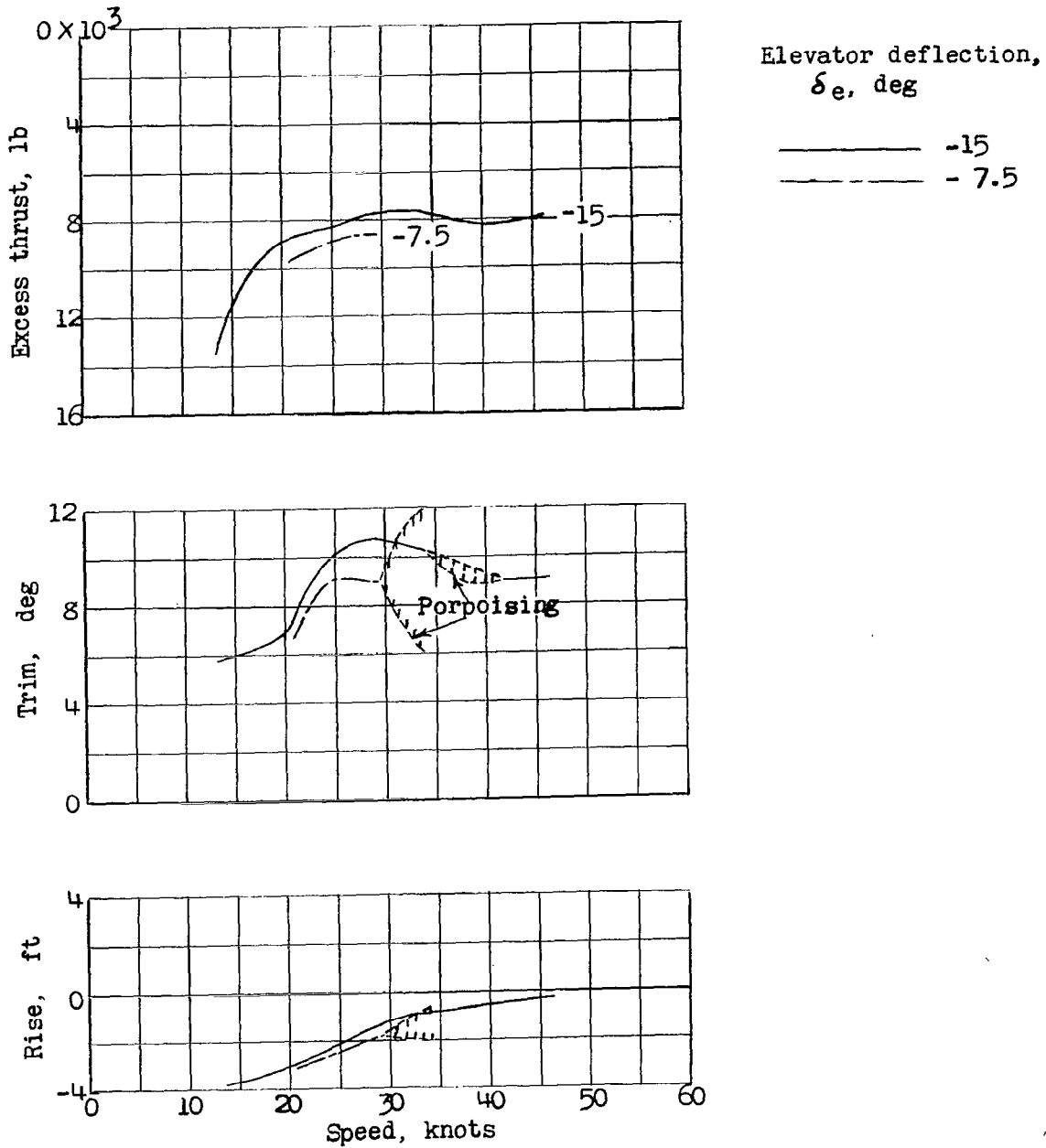
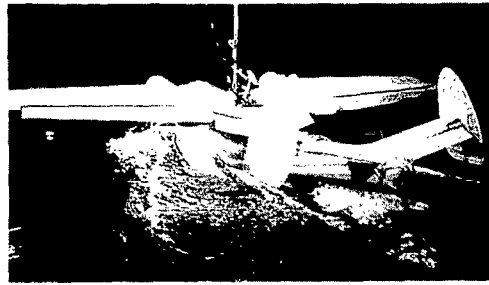
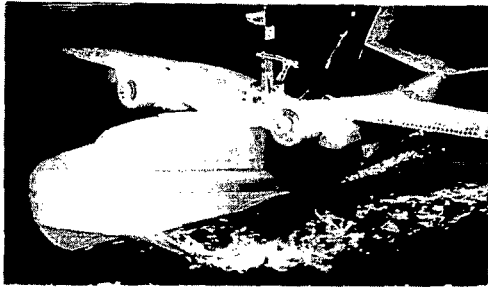
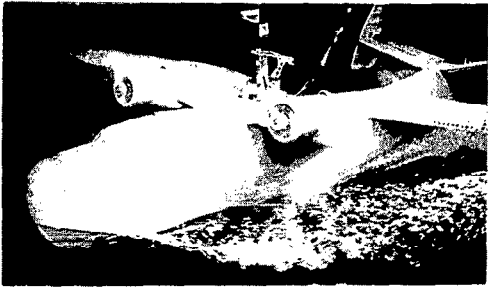


Figure 7.- Basic hull, variation of excess thrust, trim, and rise with speed. Take-off power.

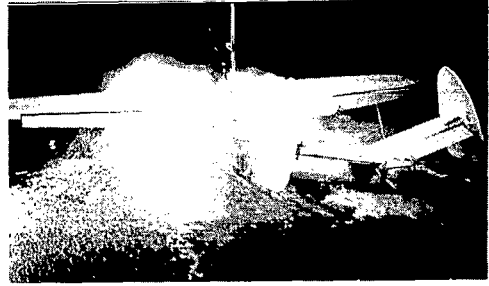
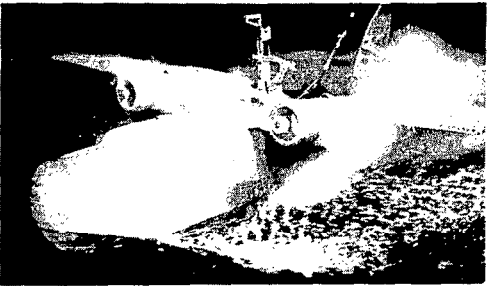
~~CONFIDENTIAL~~



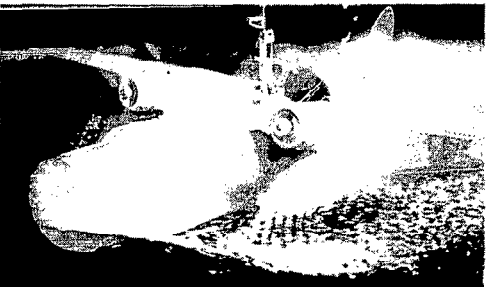
Speed, 13.6 knots; trim, 6.4°.



Speed, 14.9 knots; trim, 7.8°.



Speed, 16.8 knots; trim, 7.1°.



Speed, 18.3 knots; trim, 7.2°.

L-91705

Figure 8.- Basic-hull spray photographs.  $\delta_e = 0^\circ$ ; take-off power.

~~CONFIDENTIAL~~

~~CONFIDENTIAL~~

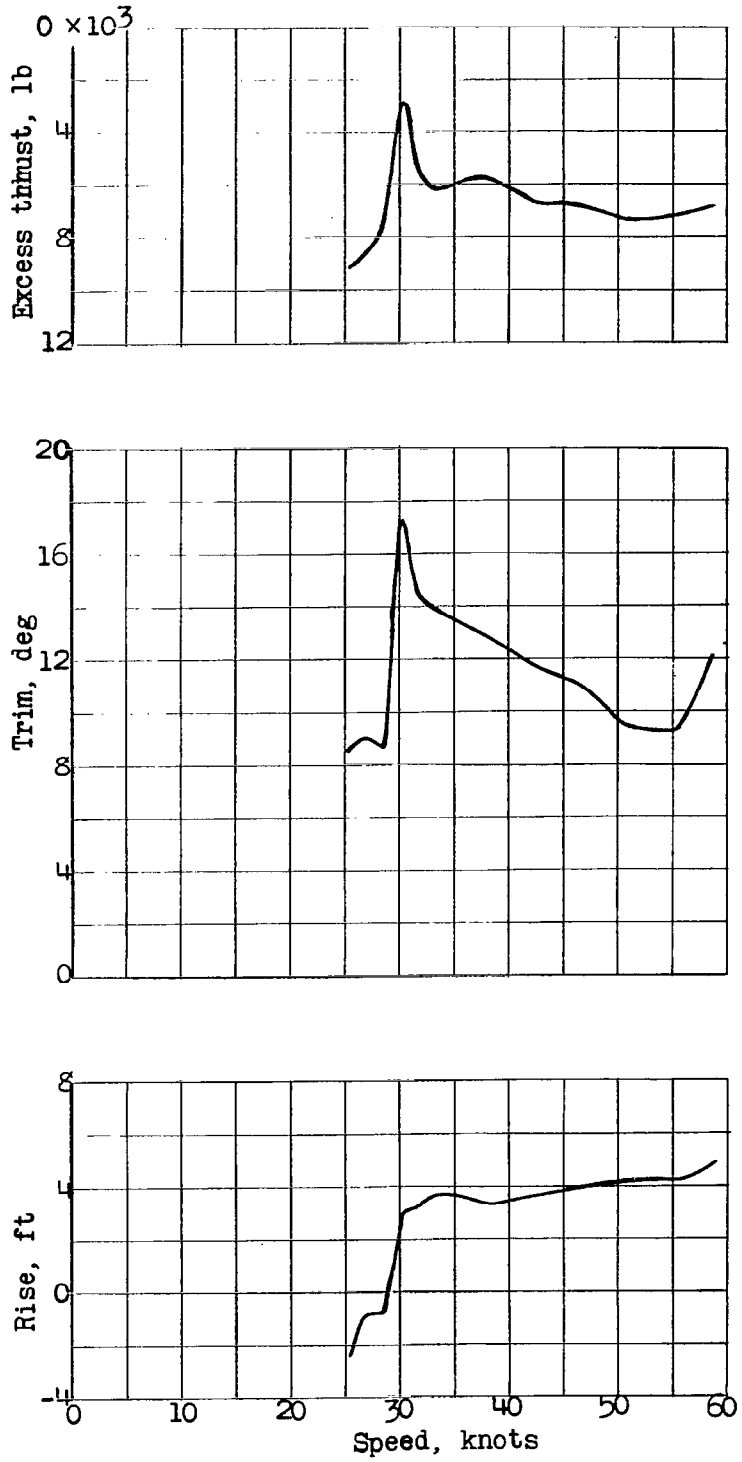


Figure 9.- Long-strut configuration; variation of excess thrust, trim, and rise with speed. Take-off power.

~~CONFIDENTIAL~~

~~CONFIDENTIAL~~

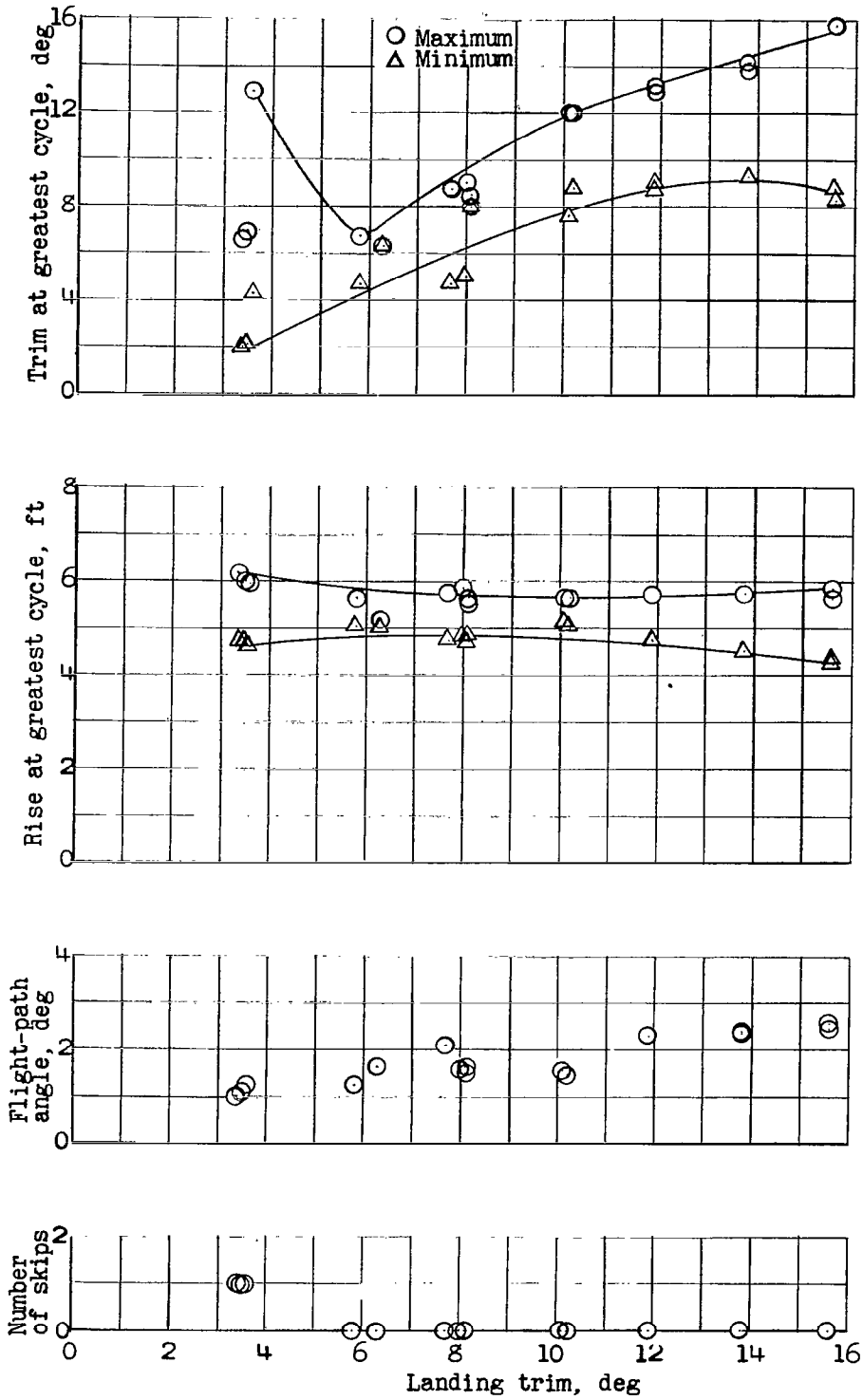


Figure 10.- Long-strut configuration; smooth-water landing characteristics. Power-off.

~~CONFIDENTIAL~~

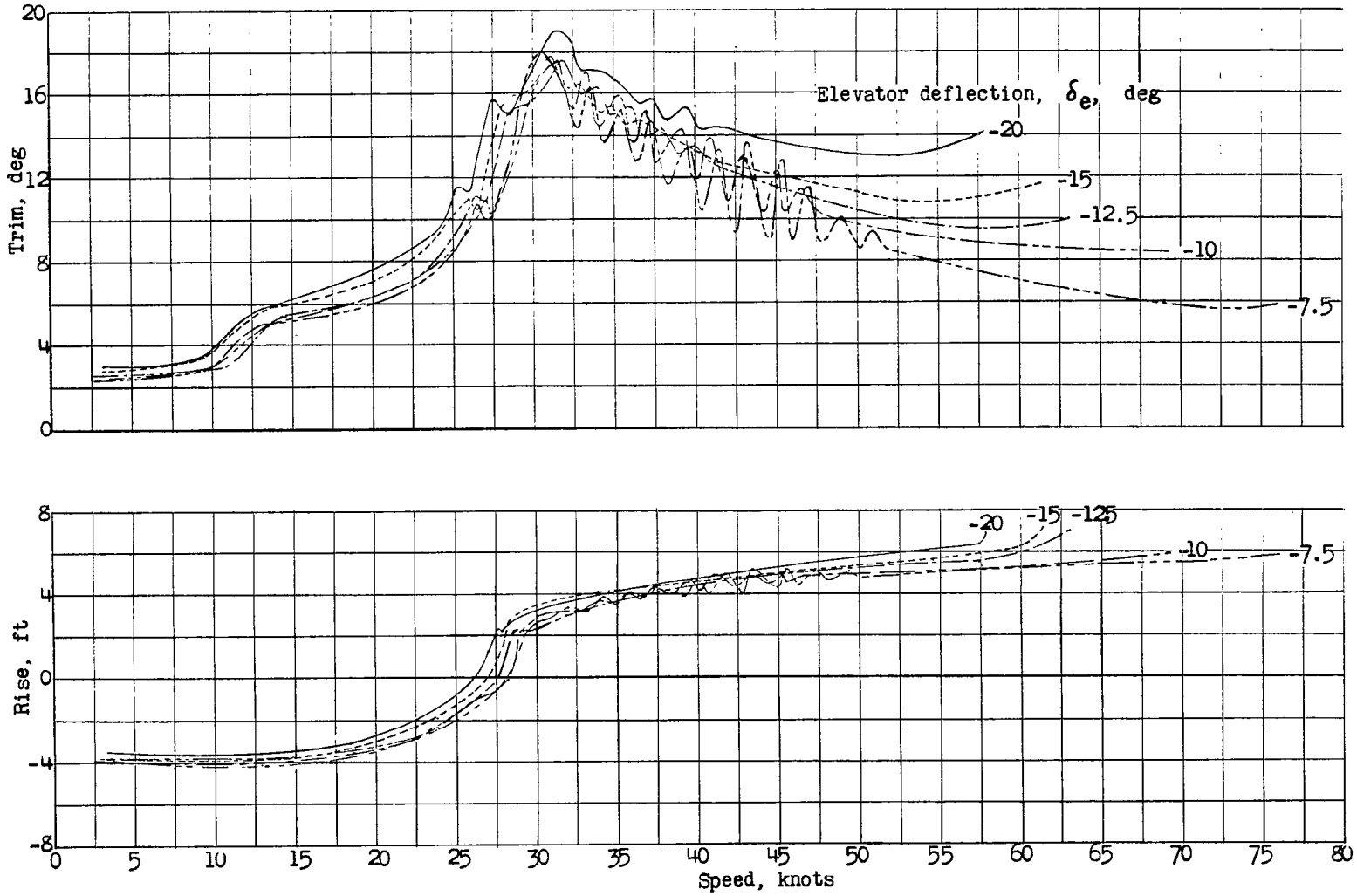


Figure 11.- Long-strut configuration; variation in trim and rise during take-offs in smooth water. Take-off power.



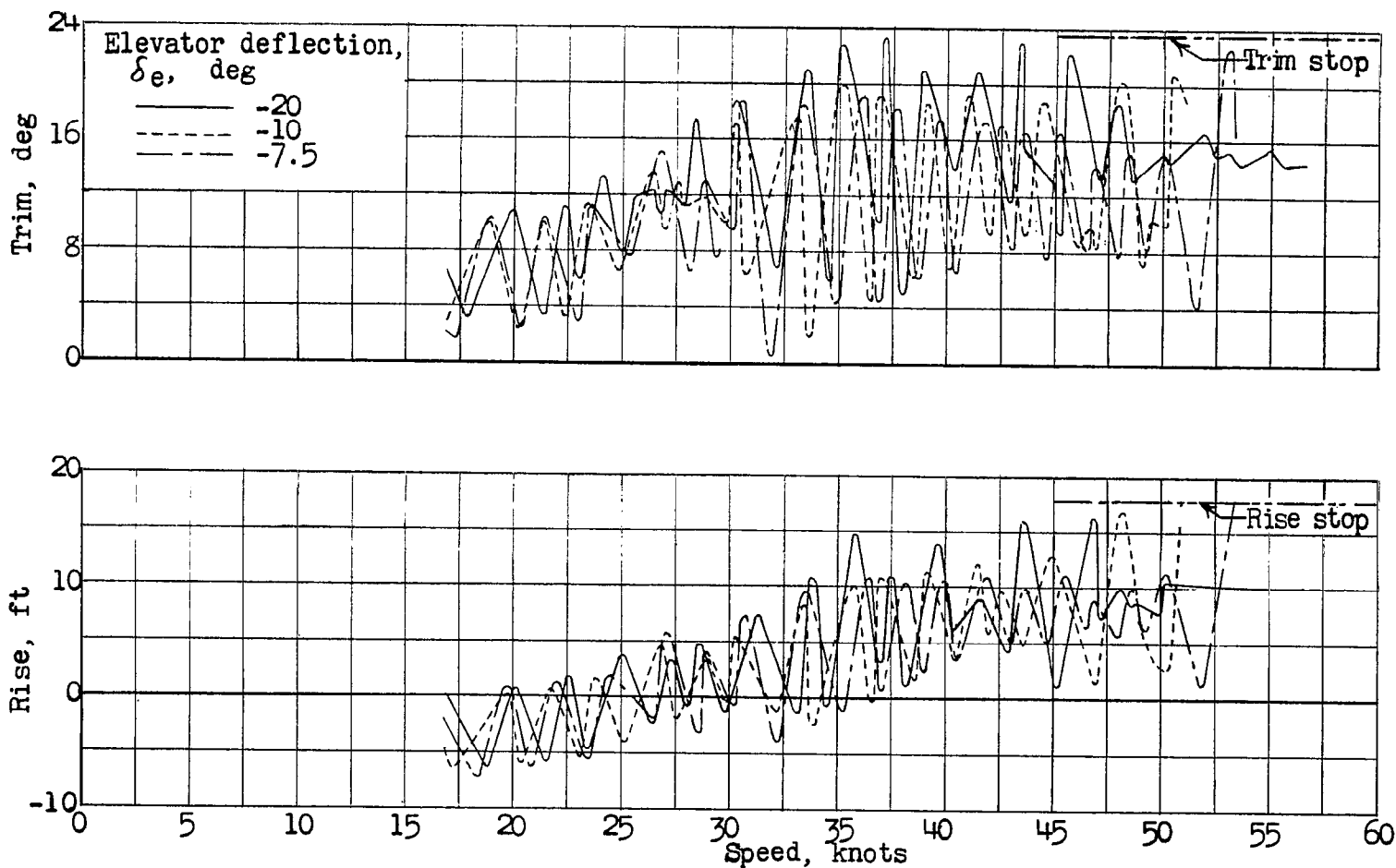
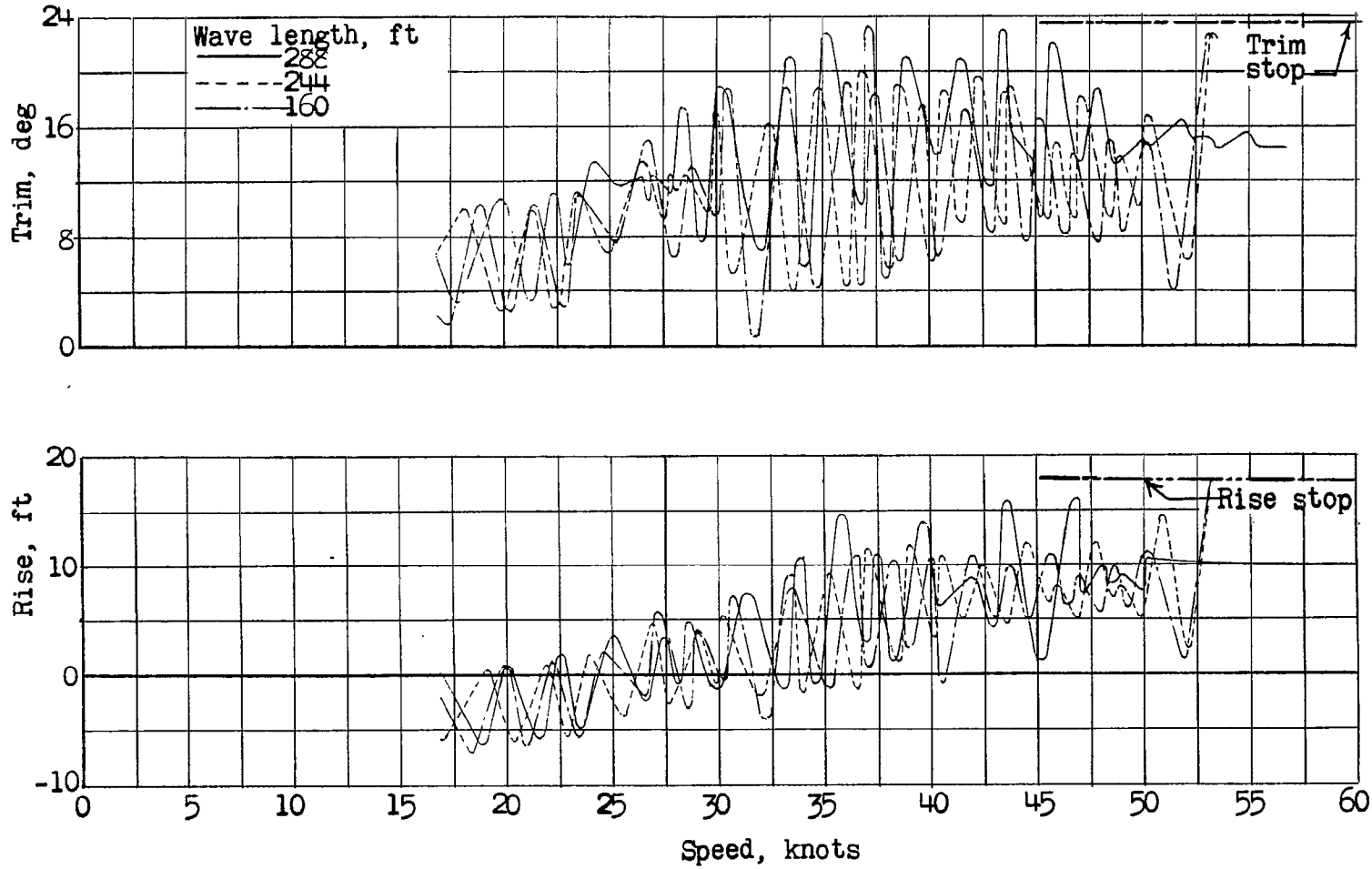


Figure 13.- Long-strut configuration; variation of trim and rise with elevator deflection during take-offs in waves 6 feet high and 288 feet long. Take-off power.

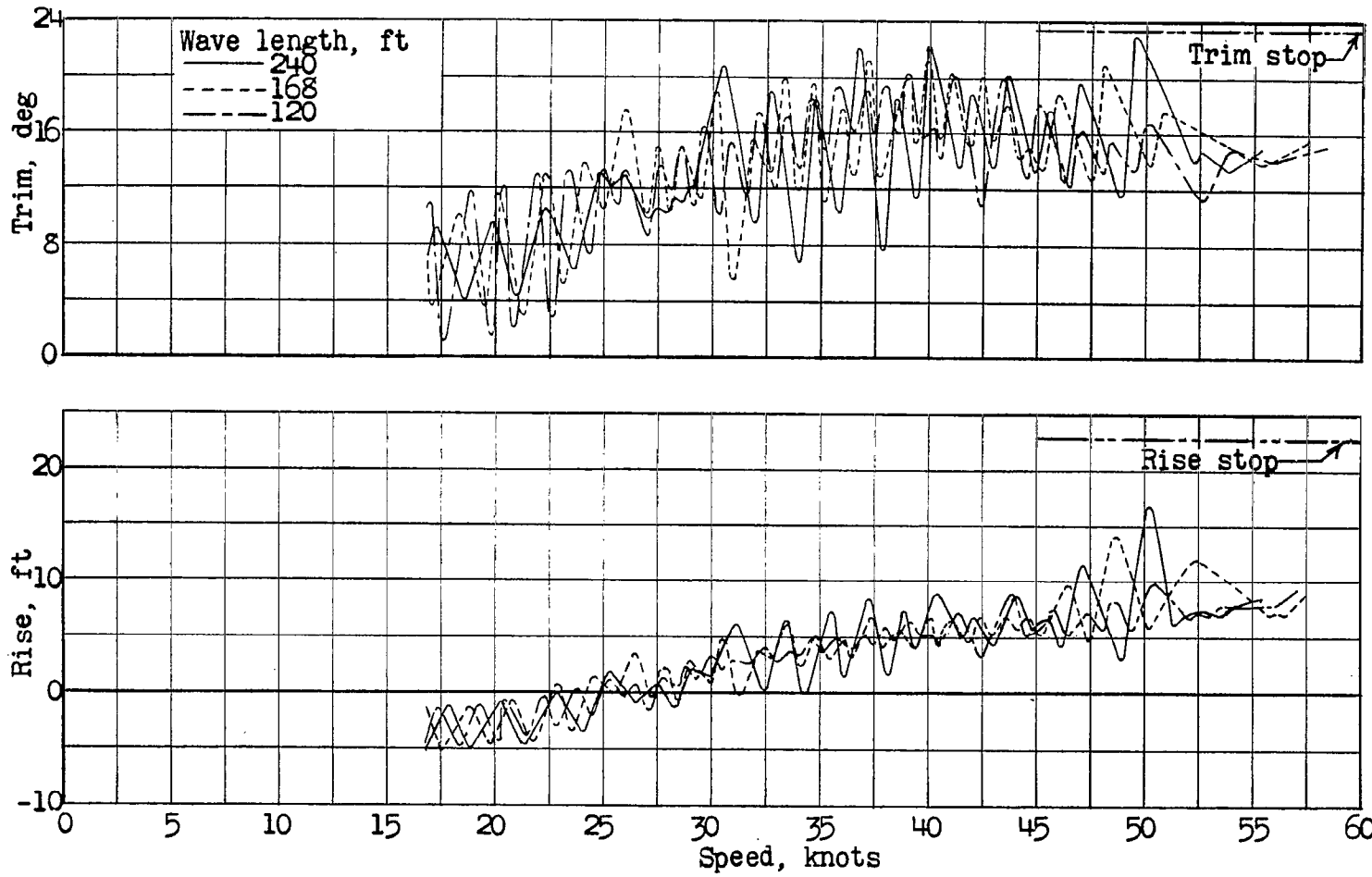
CONFIDENTIAL

CONFIDENTIAL



(a) Waves, 6 feet high.

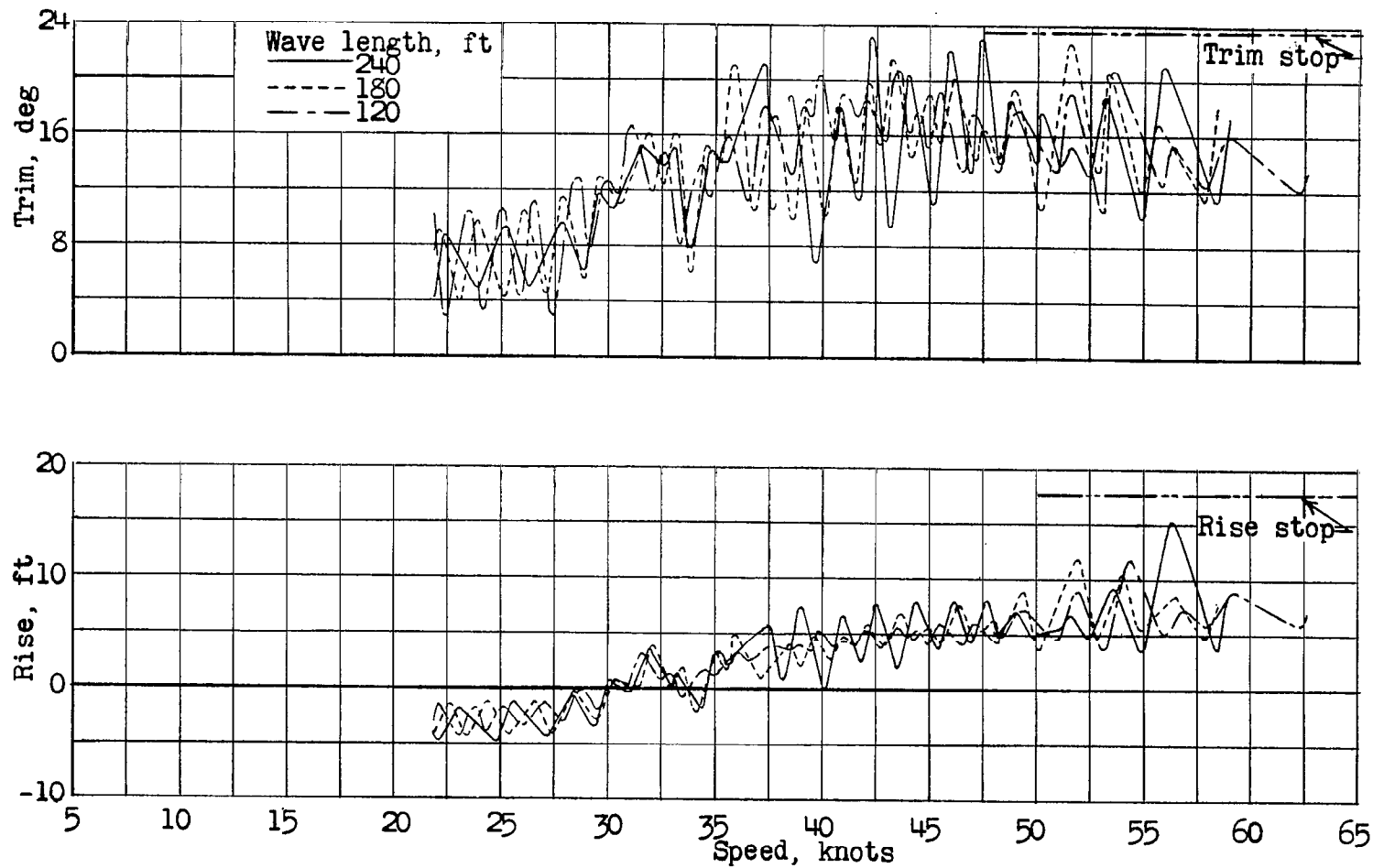
Figure 14.- Long-strut configuration; variation in trim and rise during take-offs in waves of various heights and lengths.  $\delta_e = -20^\circ$ ; take-off power.



(b) Waves, 4 feet high.

Figure 14.- Continued.

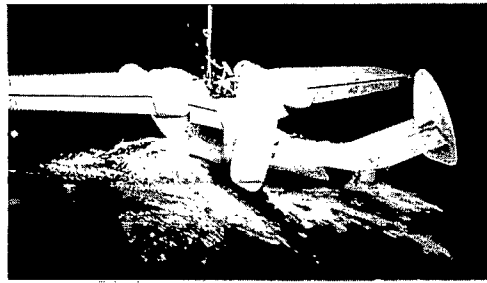
CONFIDENTIAL



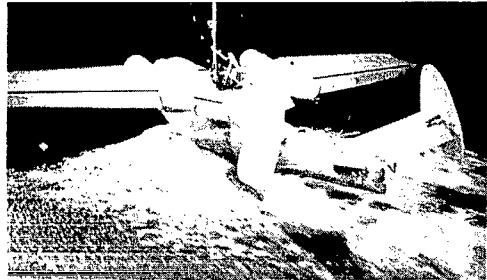
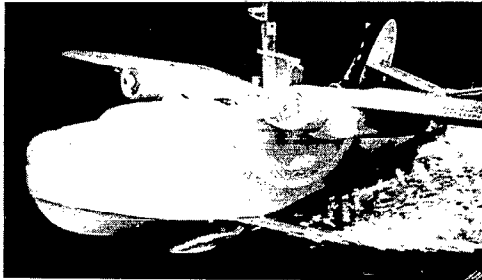
(c) Waves, 2.7 feet high.

Figure 14.- Concluded.

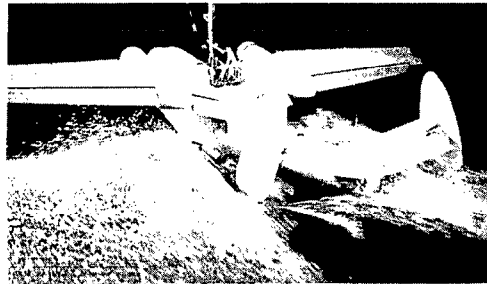
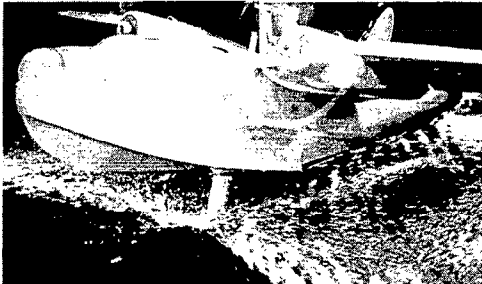
REPRODUCED FROM NACA REPORT



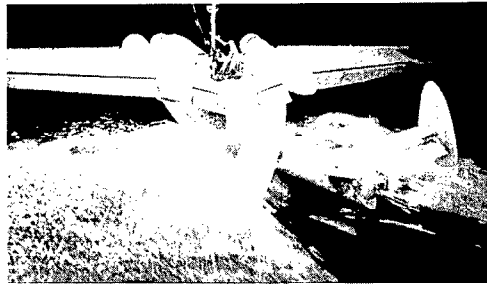
Speed, 27.6 knots; trim,  $8.3^\circ$  to  $9.7^\circ$  (unstable); rise, -1.0 ft to -1.3 ft (unstable).



Speed, 29.3 knots; trim,  $4.8^\circ$  to  $14.1^\circ$  (unstable); rise, -2.4 ft to 2.4 ft (unstable).



Speed, 31.1 knots; trim,  $14.6^\circ$ ; rise, 2.7 ft.



Speed, 33.7 knots; trim,  $16.6^\circ$ ; rise, 3.5 ft.

L-91706

Figure 15.- Long-strut-configuration spray photographs.  $\delta_e = 0^\circ$ ; take-off power.

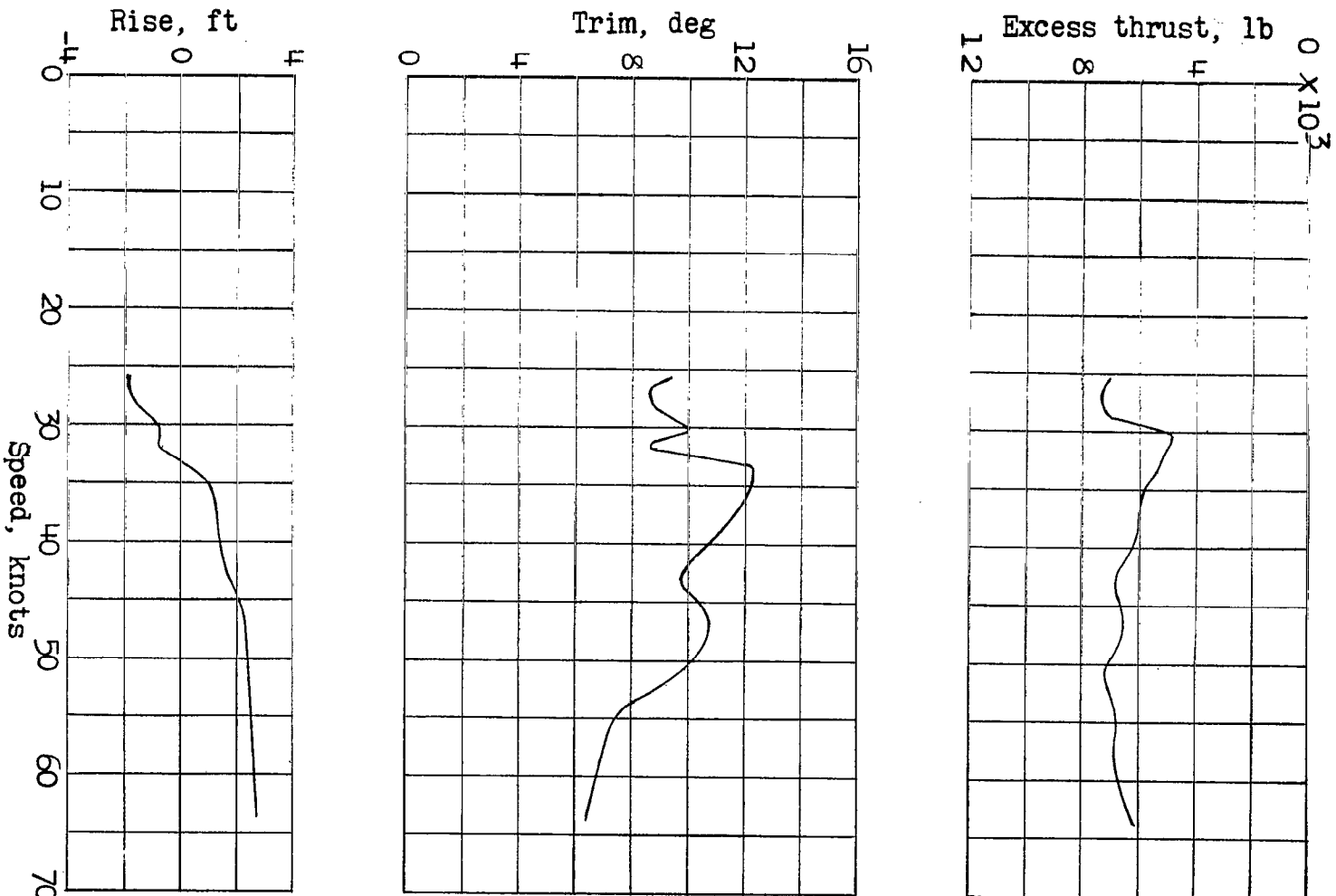


Figure 16.- Intermediate-strut configuration; variation of excess thrust, trim, and rise with speed. Take-off power.

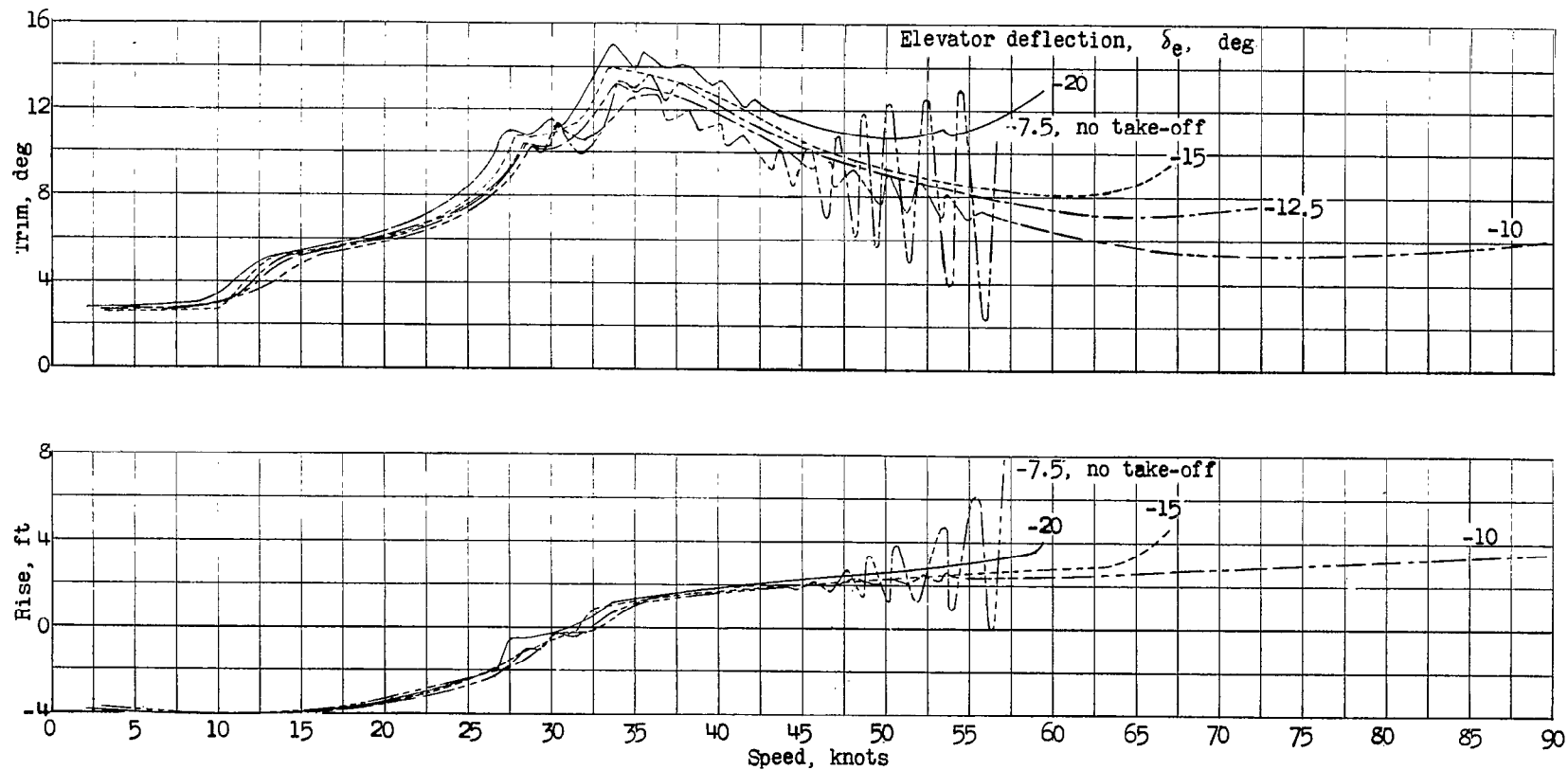
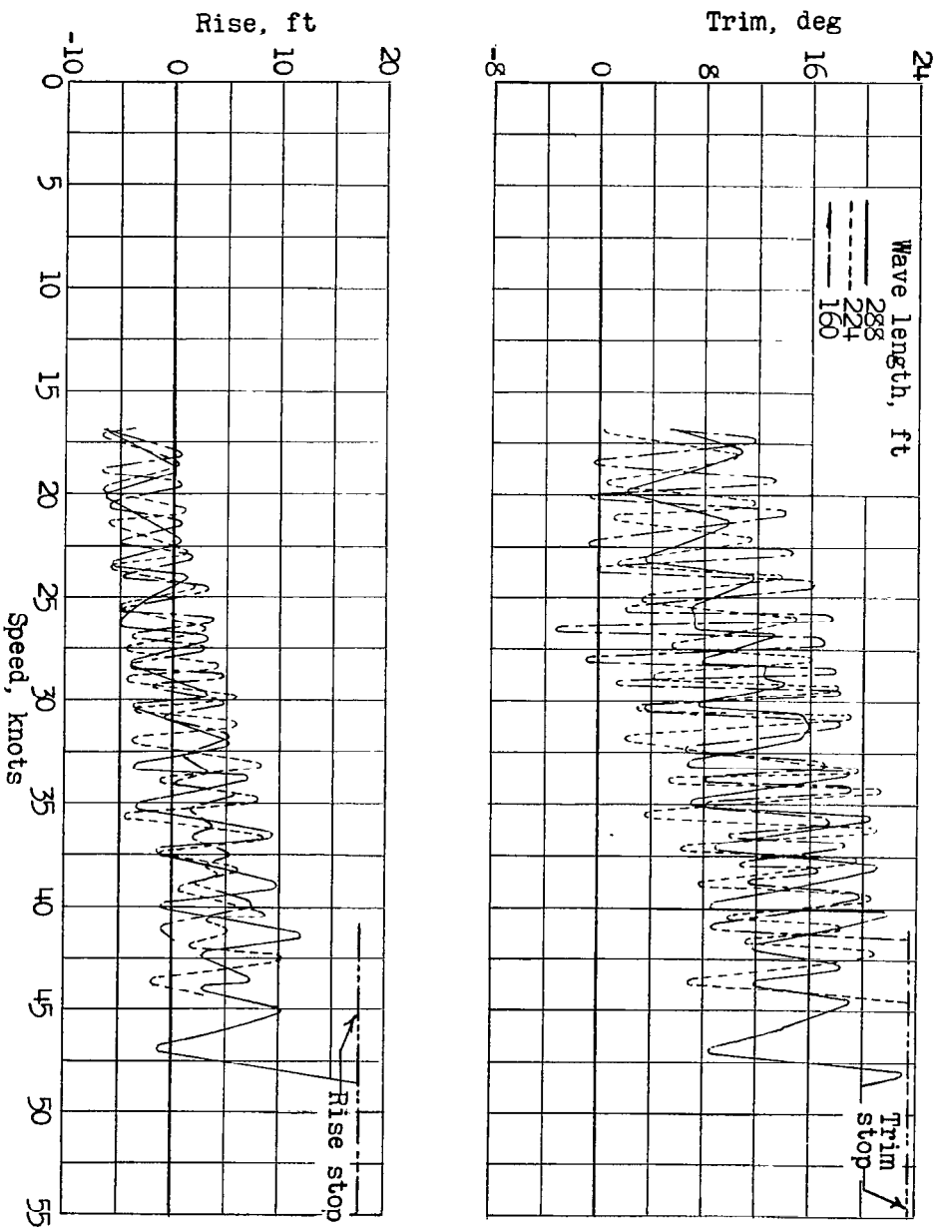
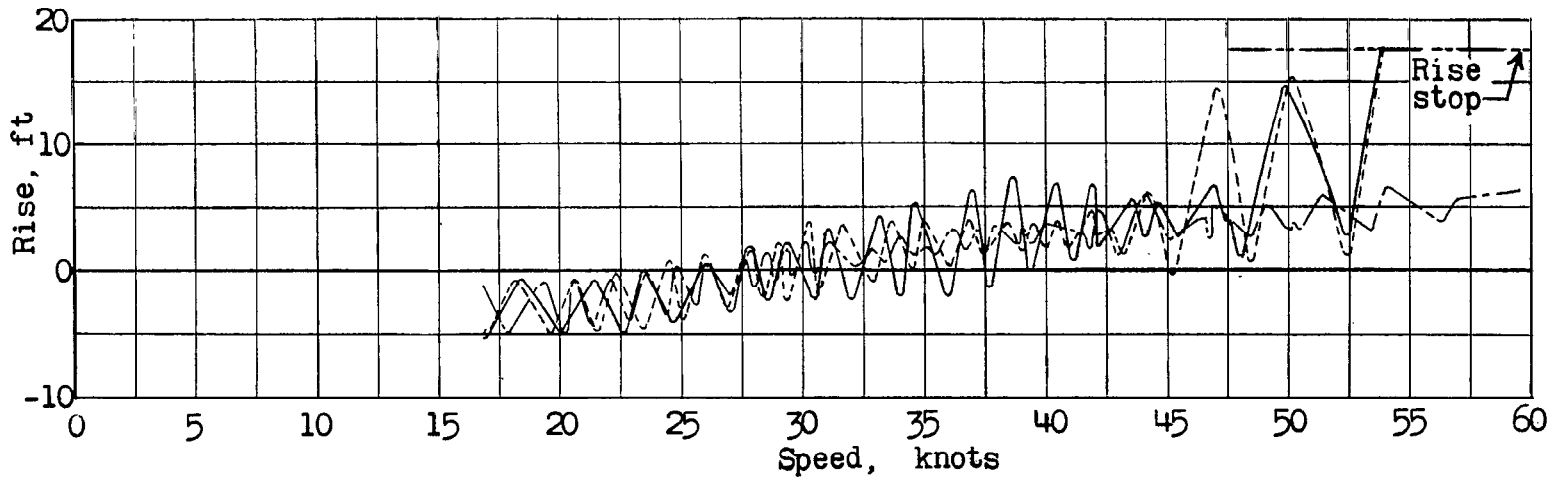
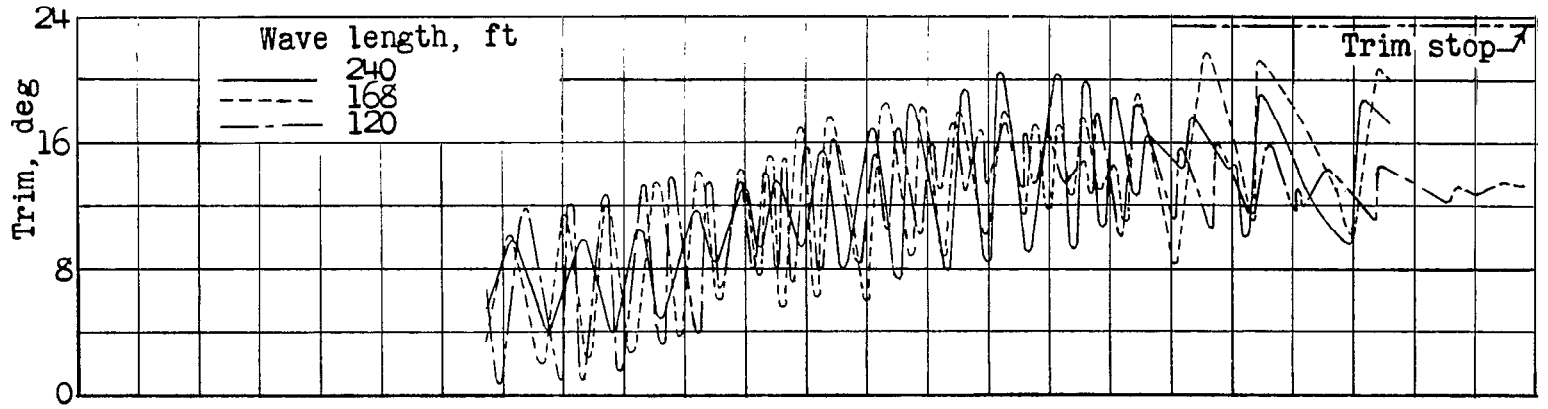


Figure 17.- Intermediate-strut configuration; variation of trim and rise during take-offs in smooth water. Take-off power.



(a) Waves, 6 feet high.

Figure 18.- Intermediate-strut configuration; variation in trim and rise during take-offs in waves of various heights and lengths.  $\delta_e = -20^\circ$ ; take-off power.

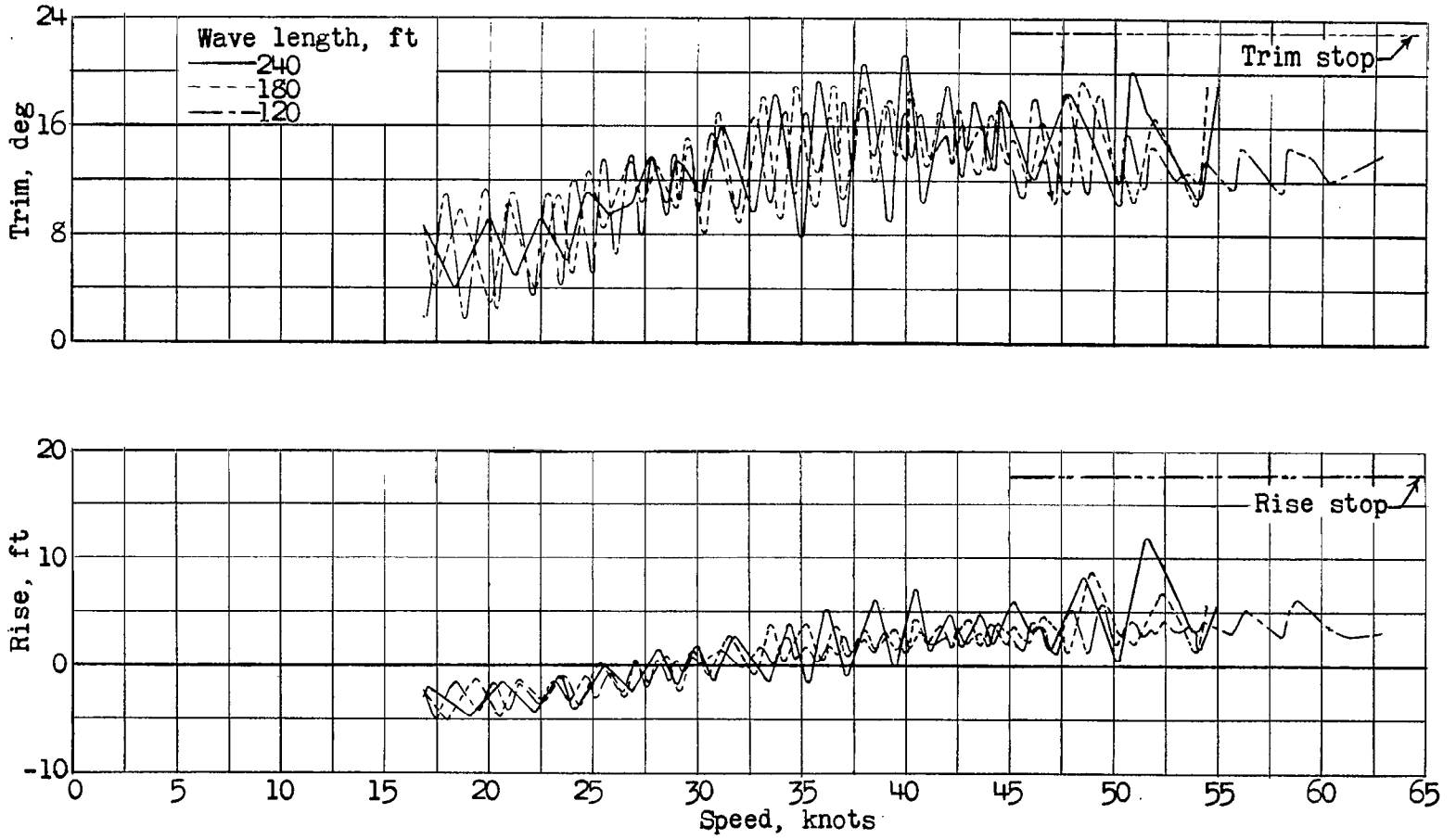


(b) Waves, 4 feet high.

Figure 18.- Continued.

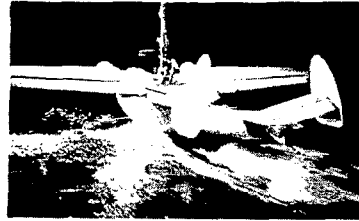
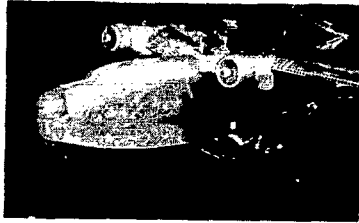
CONFIDENTIAL

CONFIDENTIAL

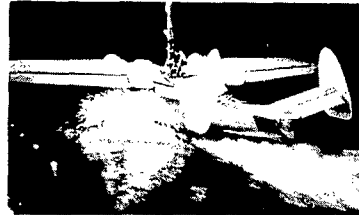
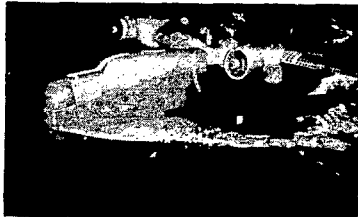


(c) Waves, 2.7 feet high.

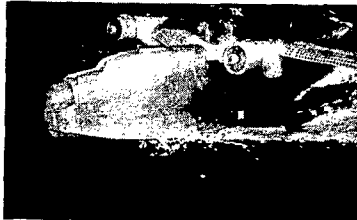
Figure 18.- Concluded.



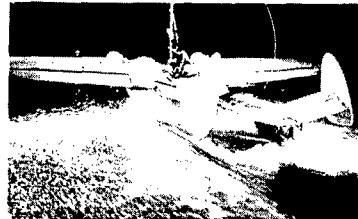
Speed, 28.5 knots; trim,  $9.0^\circ$ ; rise, -2.7 ft.



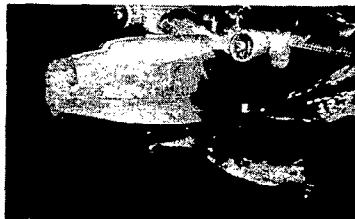
Speed, 30.5 knots; trim,  $8.5^\circ$  to  $9.8^\circ$  (unstable); rise, -2.0 ft.



Speed, 33.5 knots; trim,  $12.2^\circ$ ; rise, 1.1 ft.



Speed, 35.3 knots; trim,  $11.8^\circ$ ; rise, 1.5 ft.



Speed, 32 knots; trim,  $10.2^\circ$ ; rise, -0.2 ft.

L-91707

Figure 19.- Intermediate-strut-configuration spray photographs.  $\delta_e = 0^\circ$ ; take-off power.

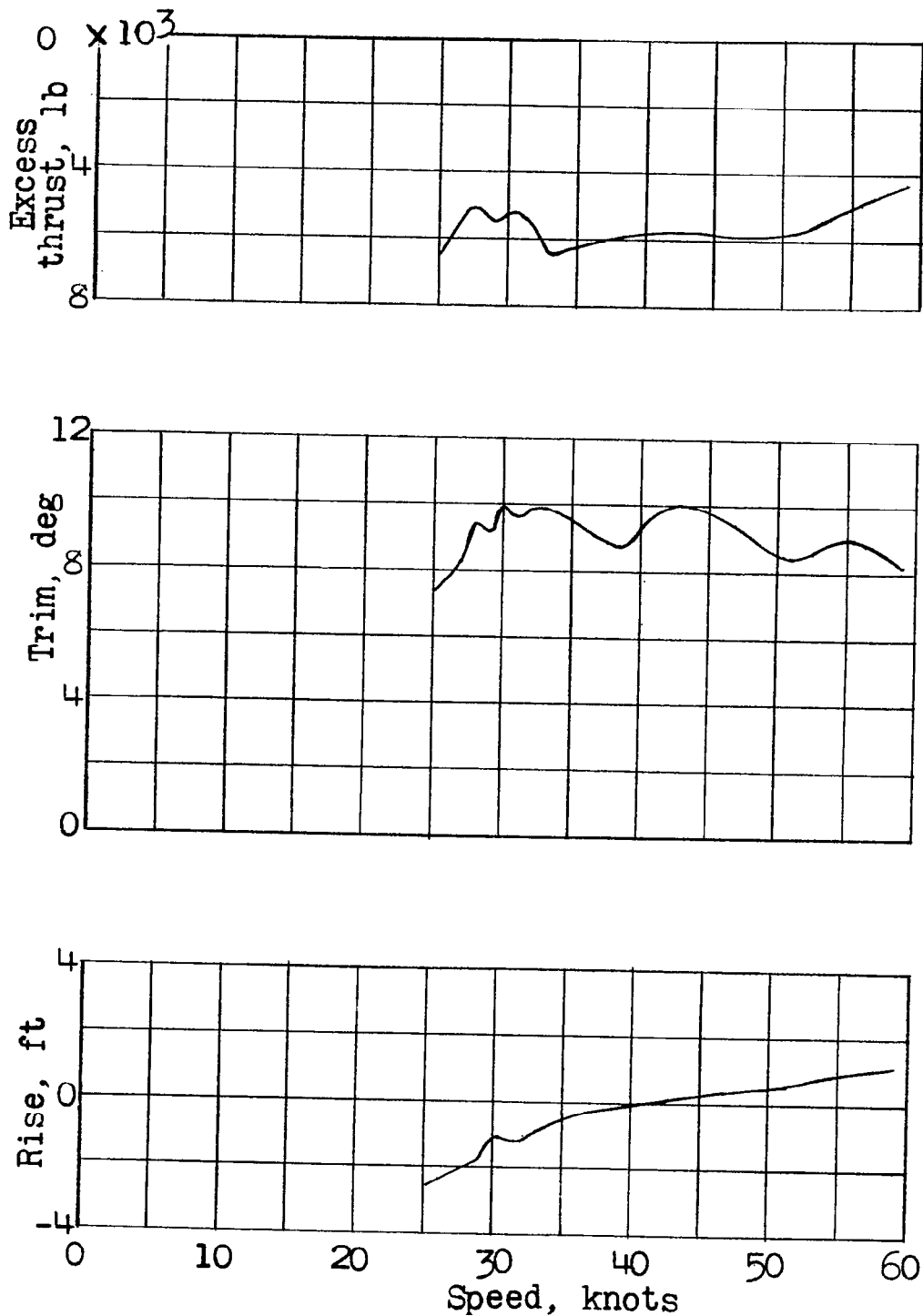


Figure 20.- Short-strut configuration; variation of excess thrust, trim, and rise with speed. Take-off power.

~~CONFIDENTIAL~~

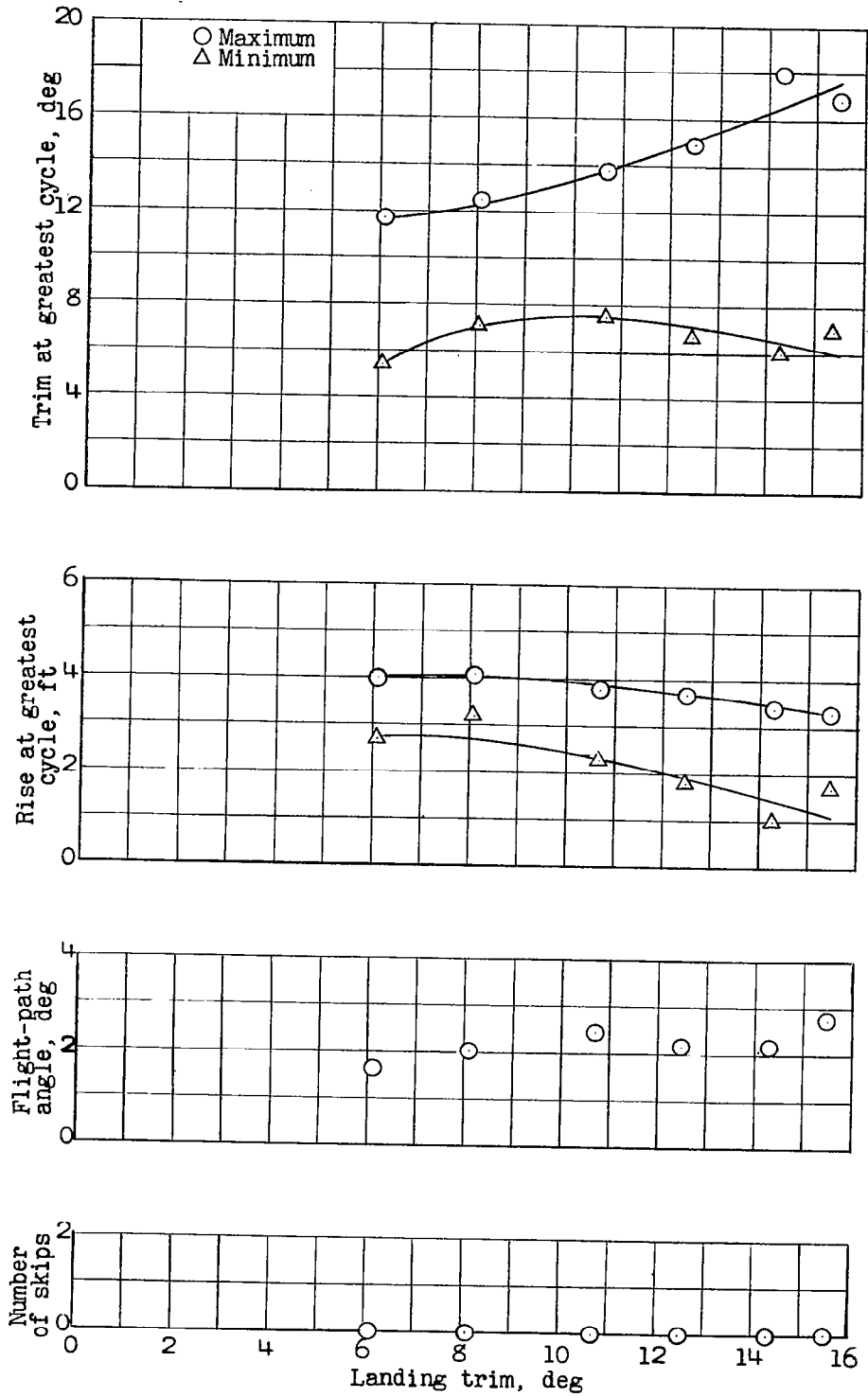


Figure 21.- Short-strut configuration; smooth-water landing characteristics. Power-off.

~~CONFIDENTIAL~~

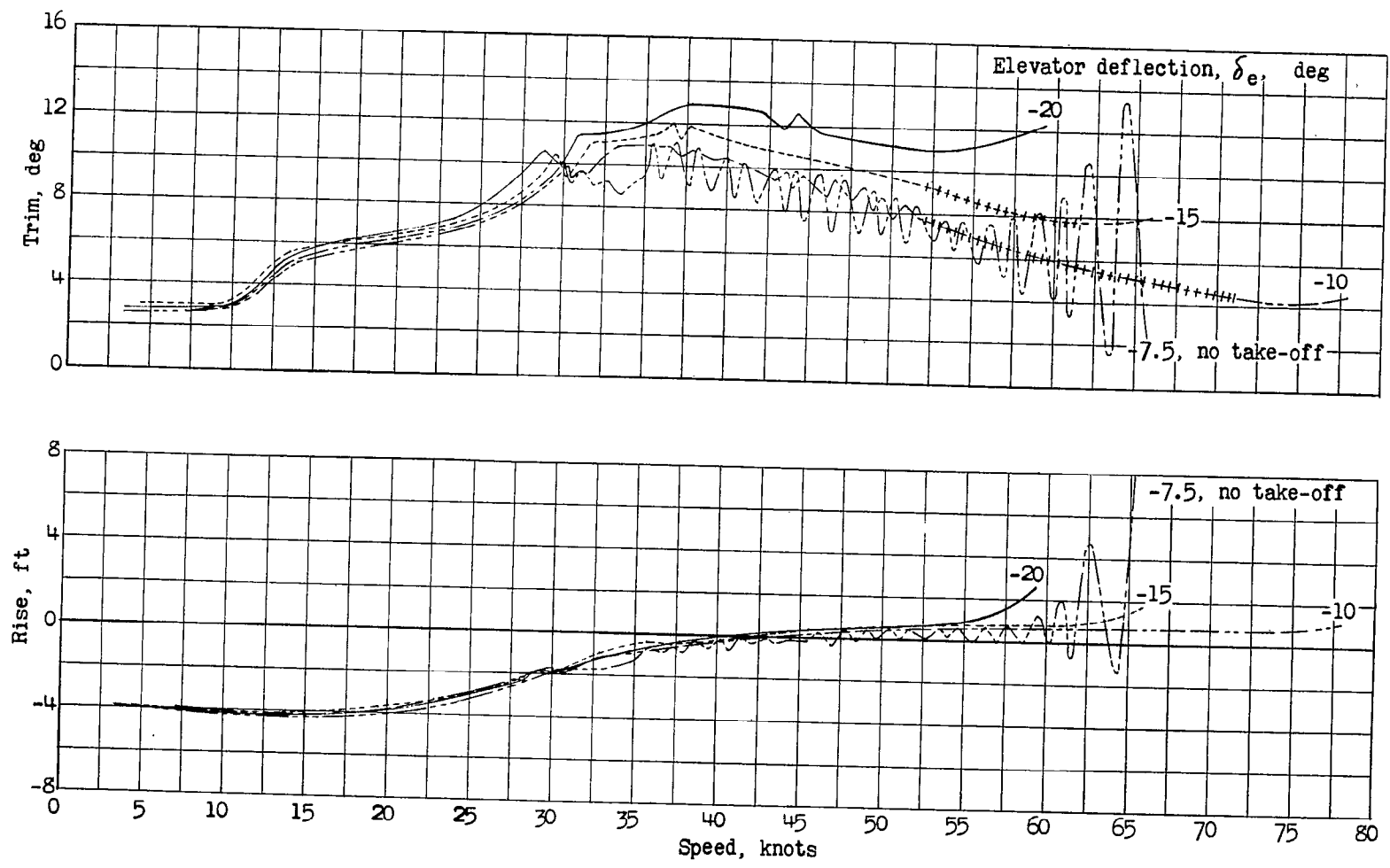
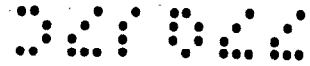
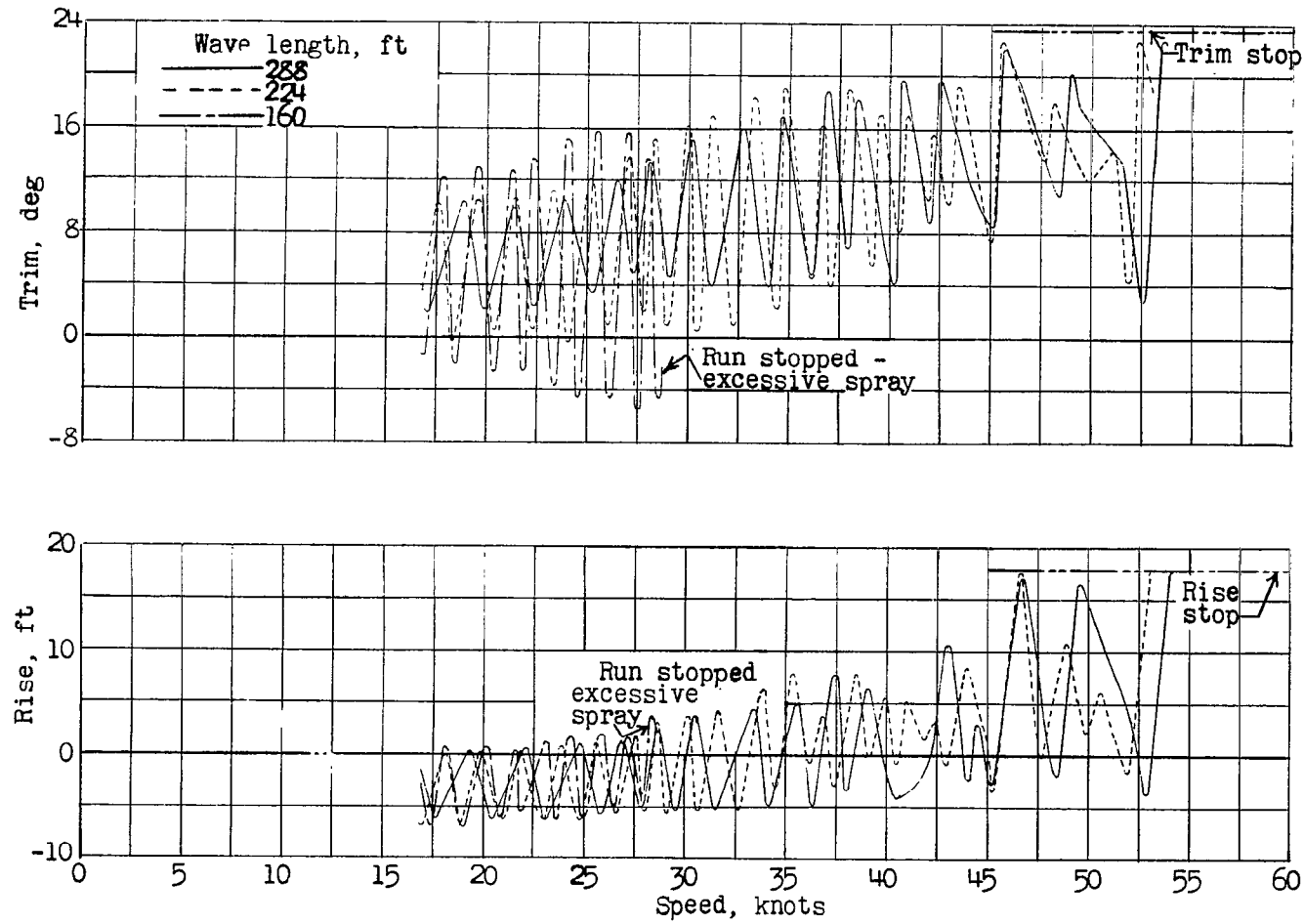
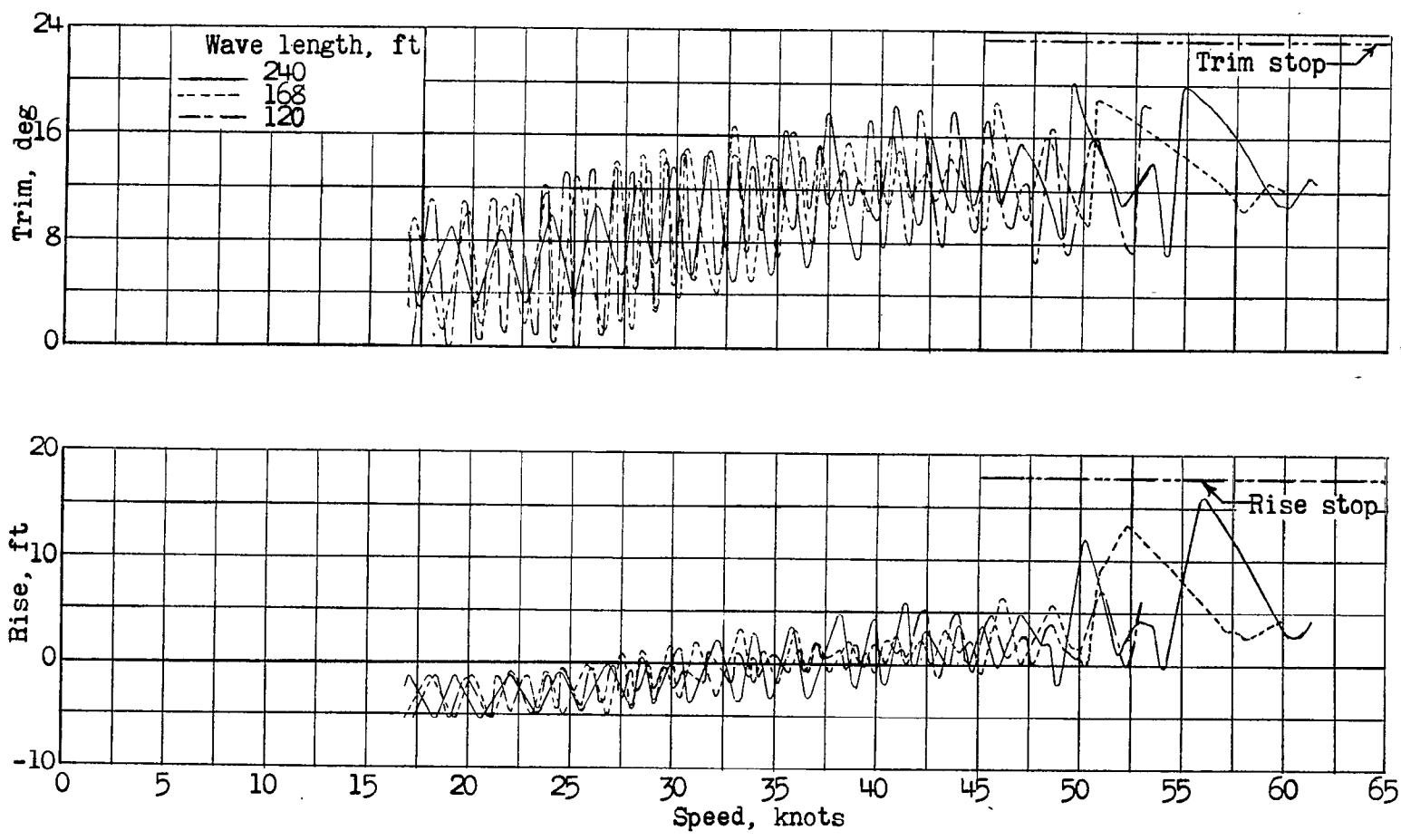


Figure 22.- Short-strut configuration; variation in trim and rise during take-offs in smooth water. Take-off power.



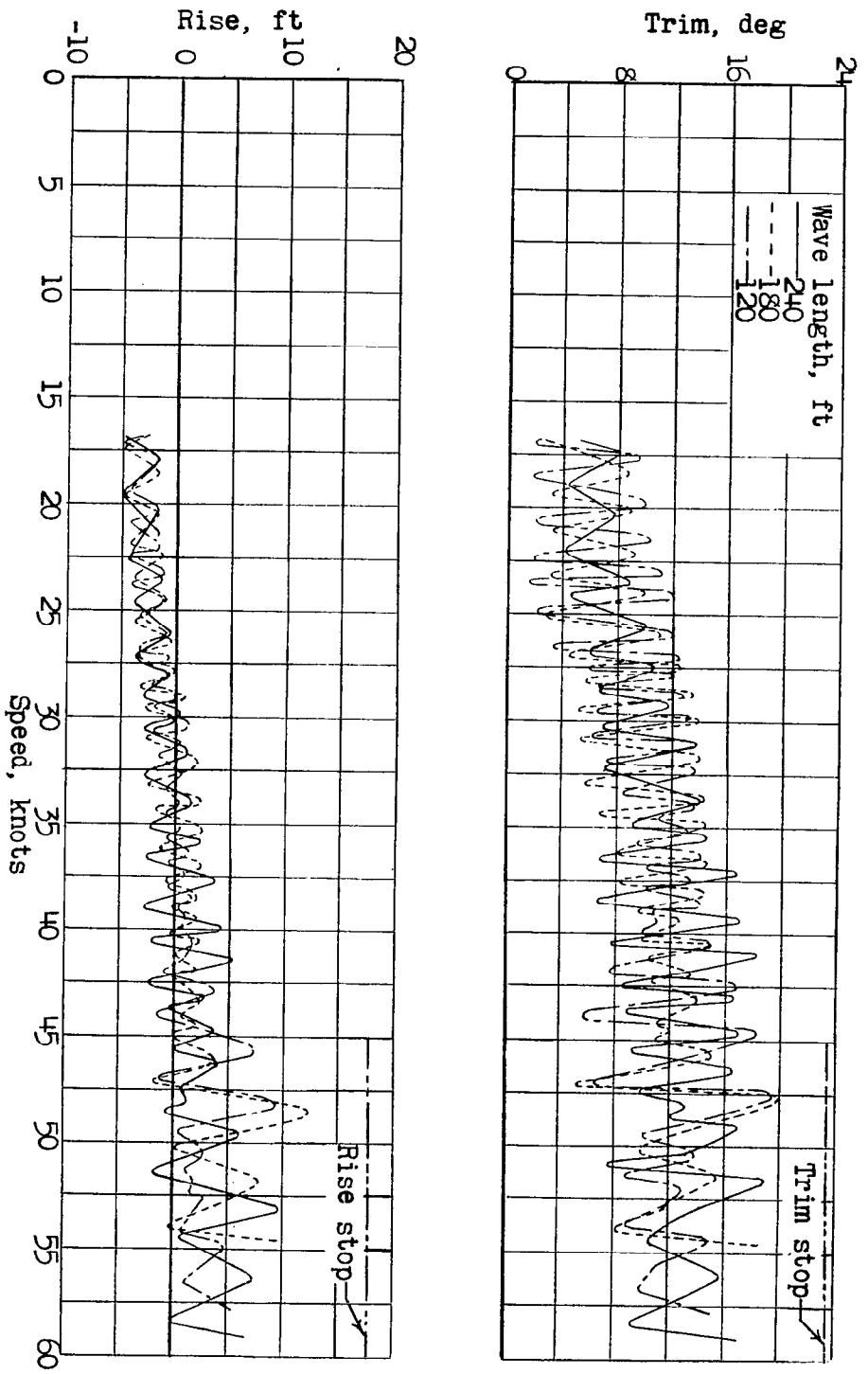
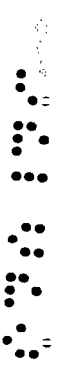
(a) Waves, 6 feet high.

Figure 23.- Short-strut configuration; variation in trim and rise during take-offs in waves of various heights and lengths.  $\delta_e = -20^\circ$ ; take-off power.

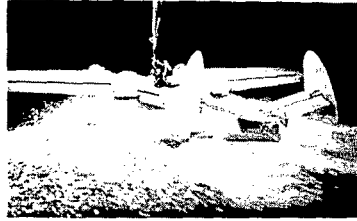


(b) Waves, 4 feet high.

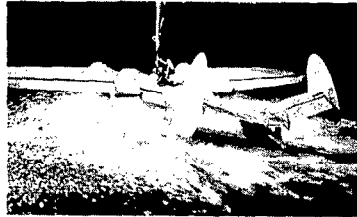
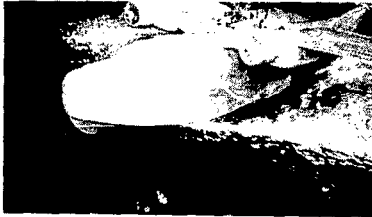
Figure 23.- Continued.



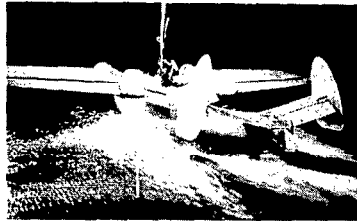
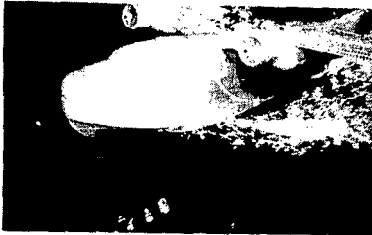
(c) Waves, 2.7 feet high.  
Figure 23.- Concluded.



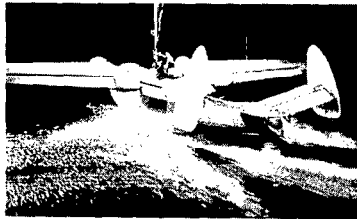
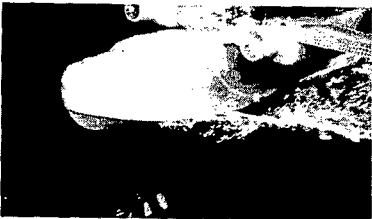
Speed, 27.1 knots; trim,  $7.9^\circ$ ; rise, -2.5 ft.



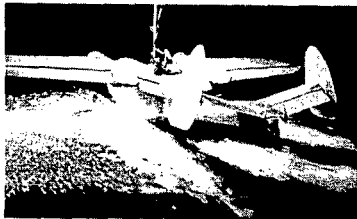
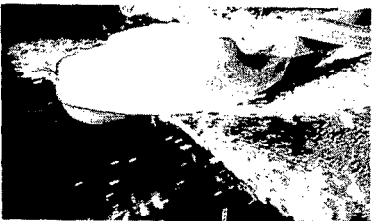
Speed, 28.6 knots; trim,  $8.6^\circ$ ; rise, -2.1 ft.



Speed, 30.2 knots; trim,  $9.4^\circ$ ; rise, -1.4 ft.



Speed, 32 knots; trim,  $9.1^\circ$ ; rise, -1.3 ft.



Speed, 33.5 knots; trim,  $9.7^\circ$ ; rise, -0.9 ft.

Figure 24.- Short-strut-configuration spray photographs.  $\delta_e = 0^\circ$ ; take-off power.

L-91708

~~CONFIDENTIAL~~

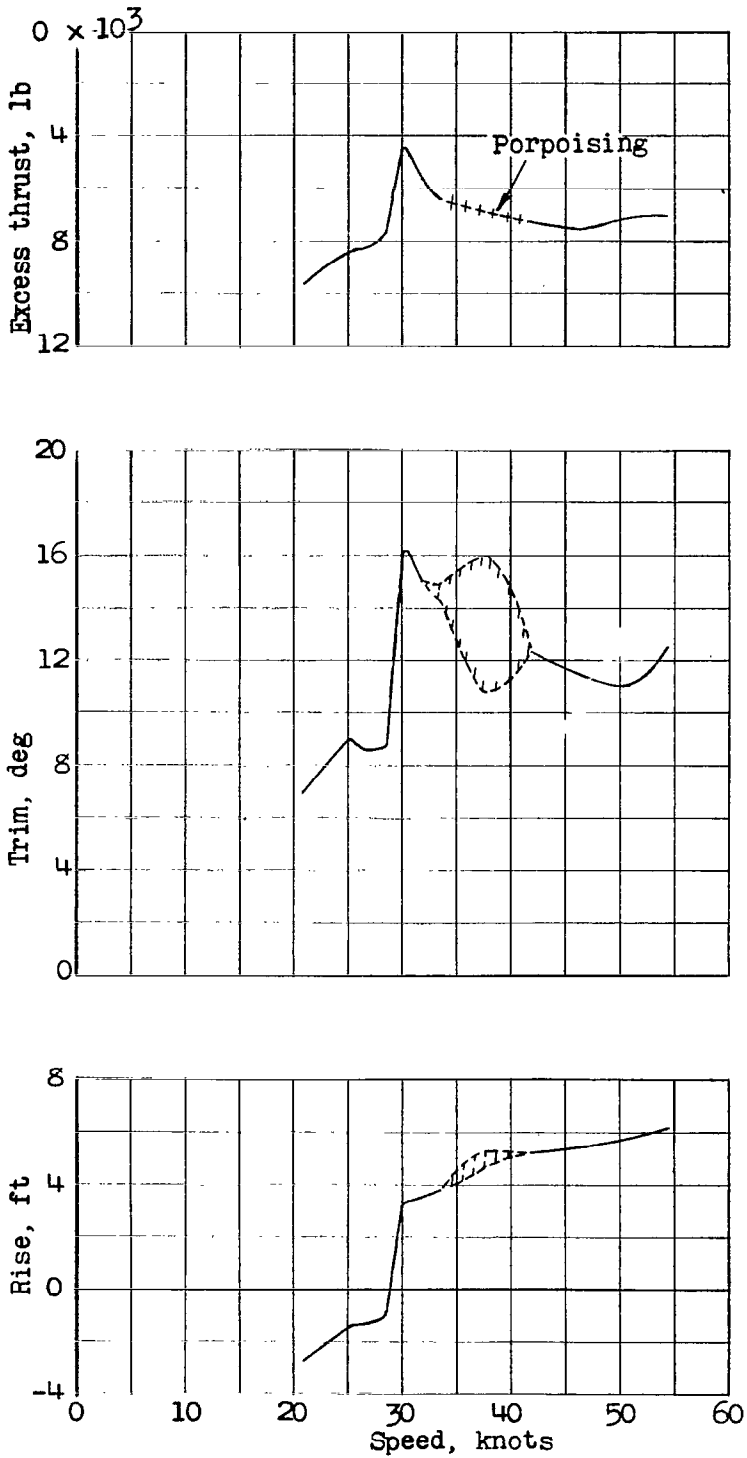


Figure 25.- Aft-ski configuration (long strut); variation of excess thrust, trim, and rise with speed. Take-off power.

~~CONFIDENTIAL~~

~~CONFIDENTIAL~~

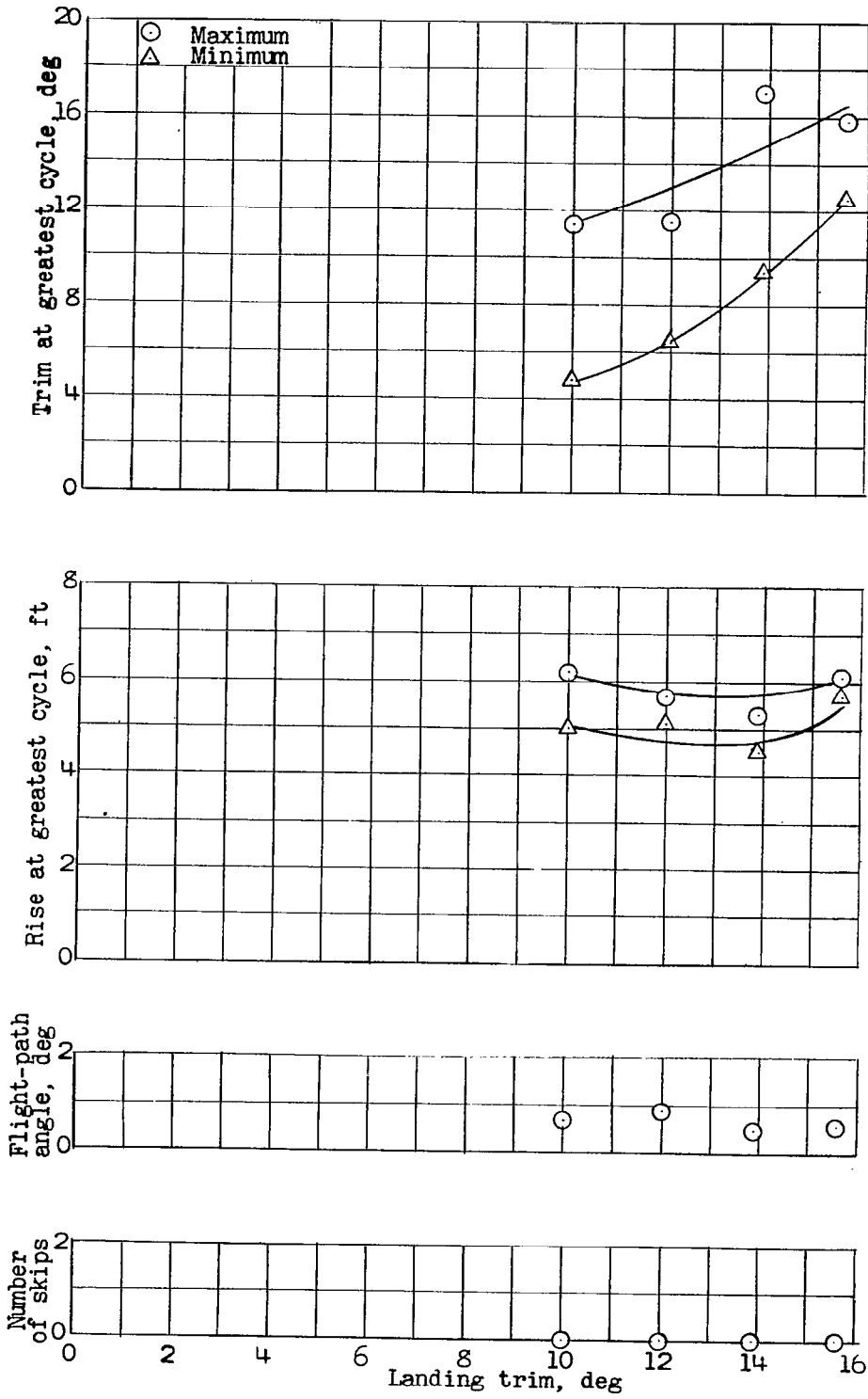


Figure 26.- Aft-ski configuration (long strut); smooth-water landing characteristics. Power-off.

~~CONFIDENTIAL~~

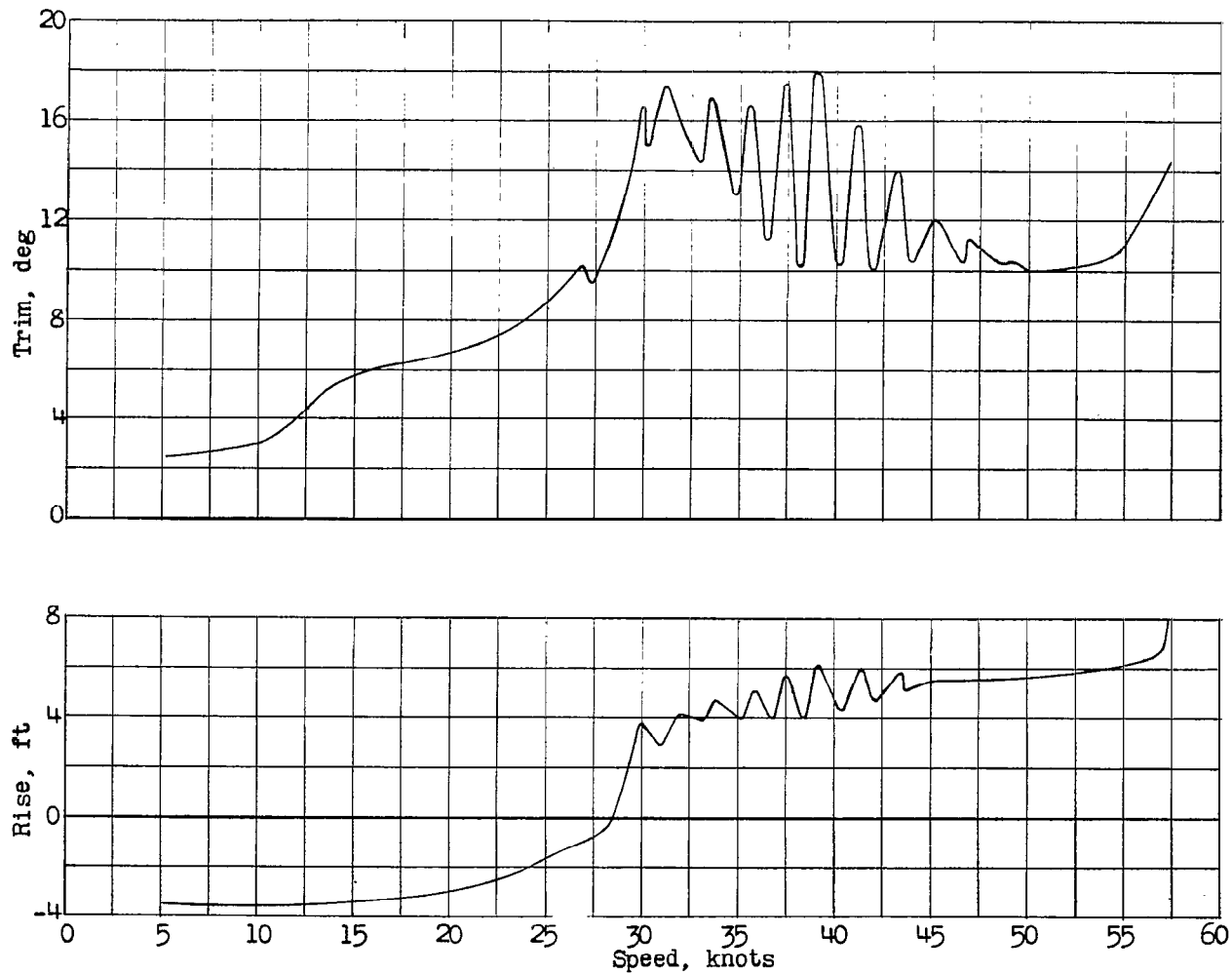


Figure 27.- Aft-ski configuration (long strut); variation in trim and rise during a take-off in smooth water.  $\delta_e = -20^\circ$ ; take-off power.

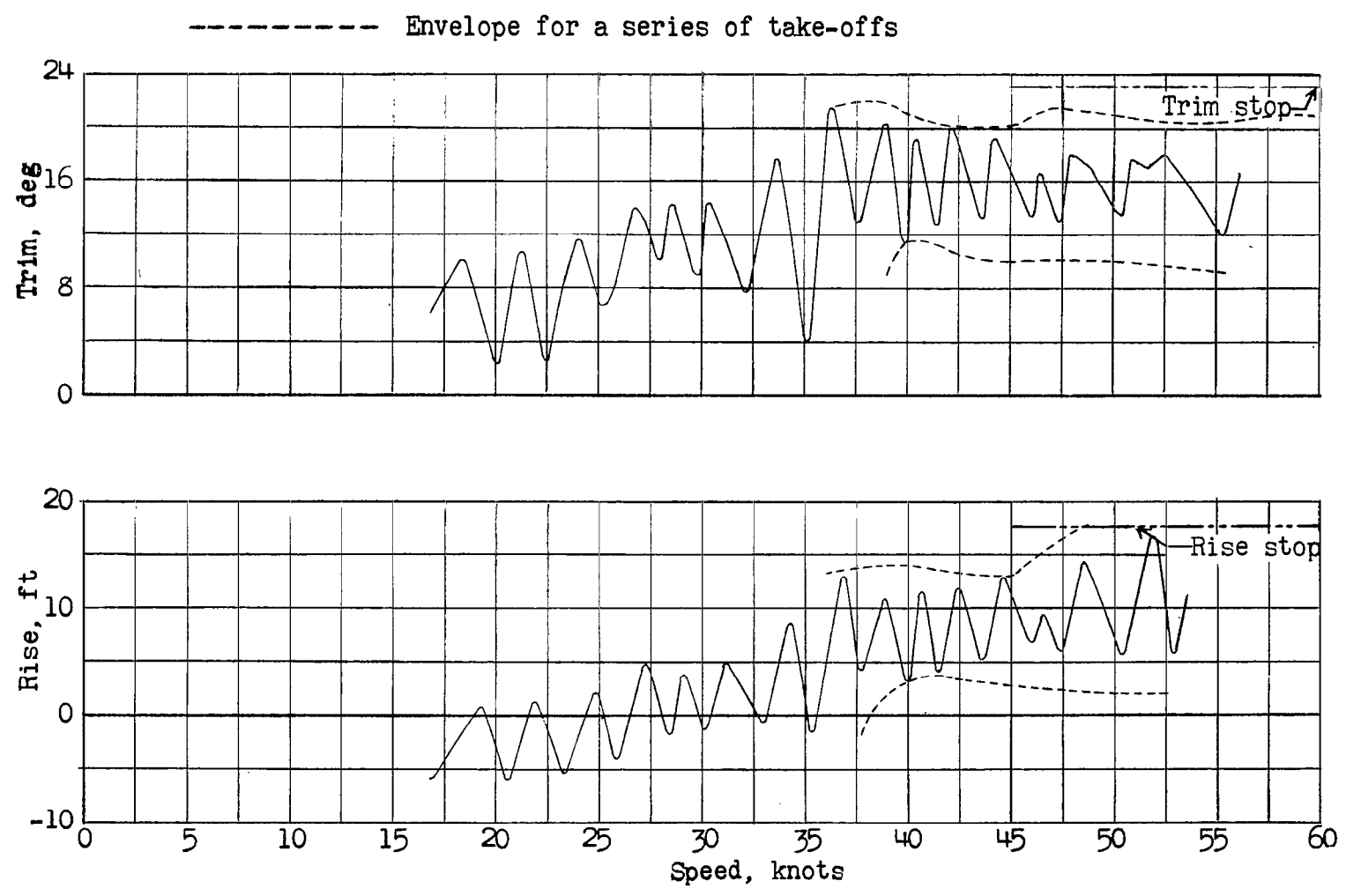
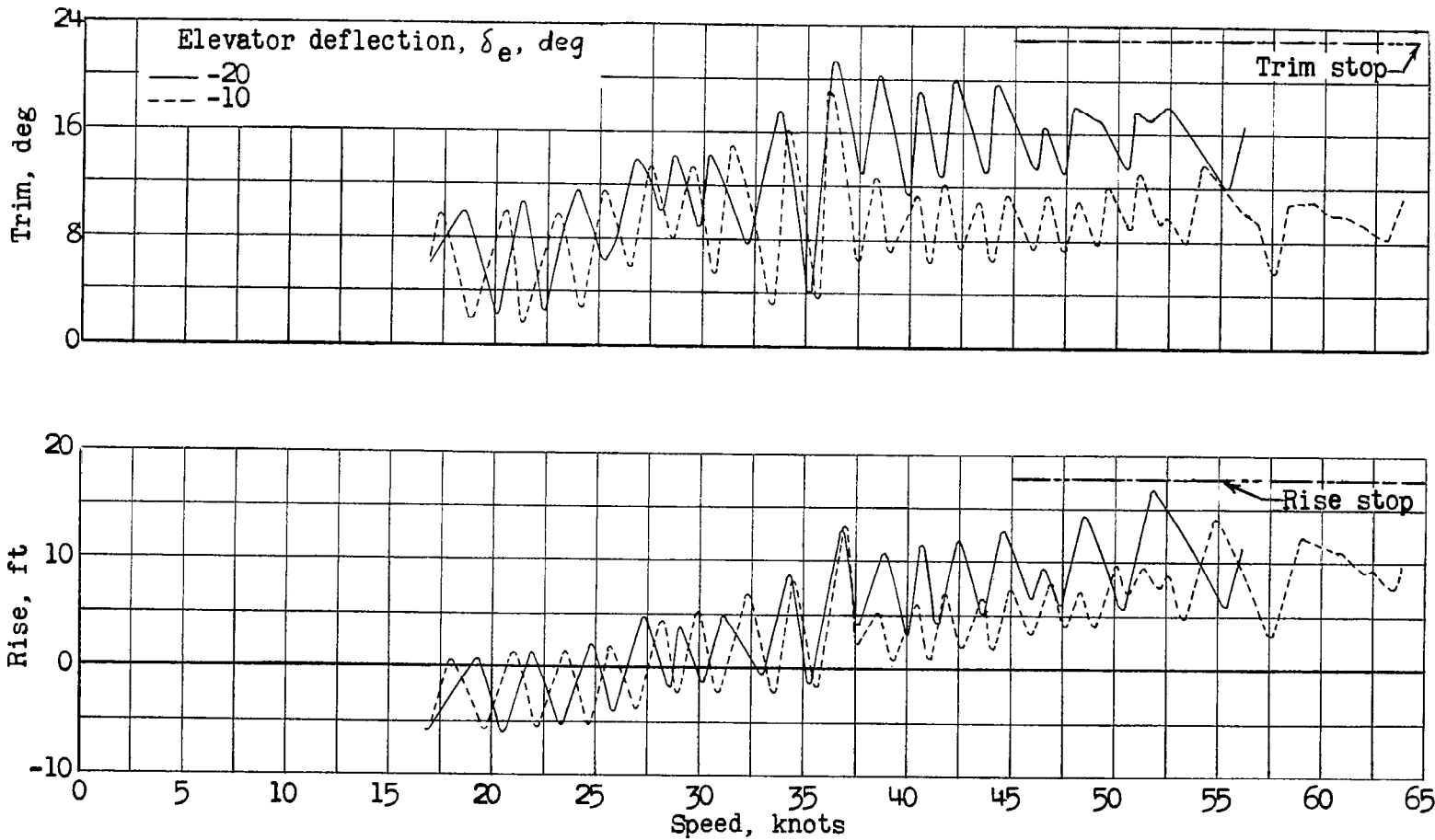


Figure 28.- Aft-ski configuration (long strut); variation in trim and rise during take-offs in waves 6 feet high and 288 feet long.  $\delta_e = -20^\circ$ ; take-off power.

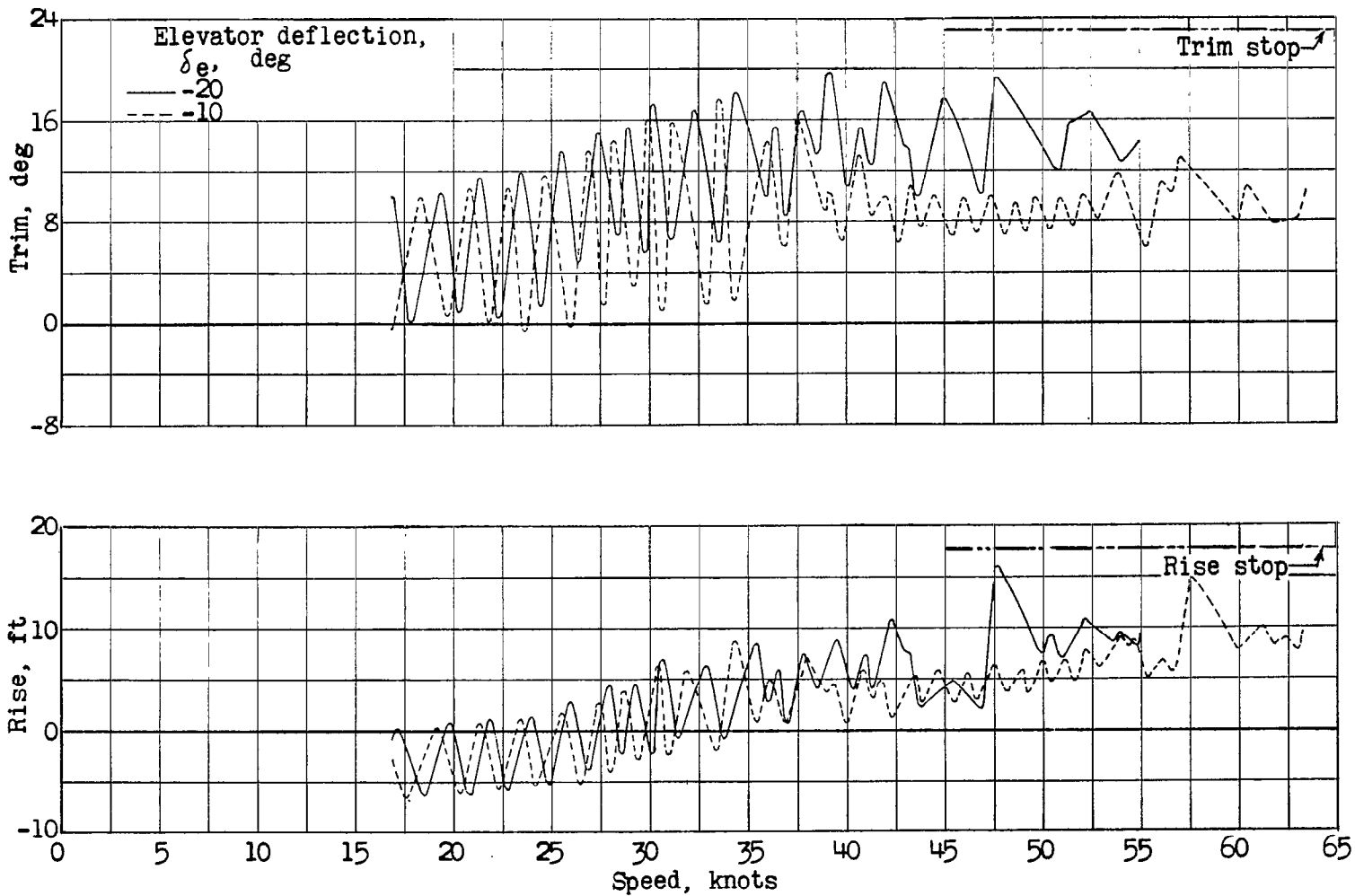
REPRODUCED FROM NACA REPORT

REPRODUCED FROM NACA REPORT



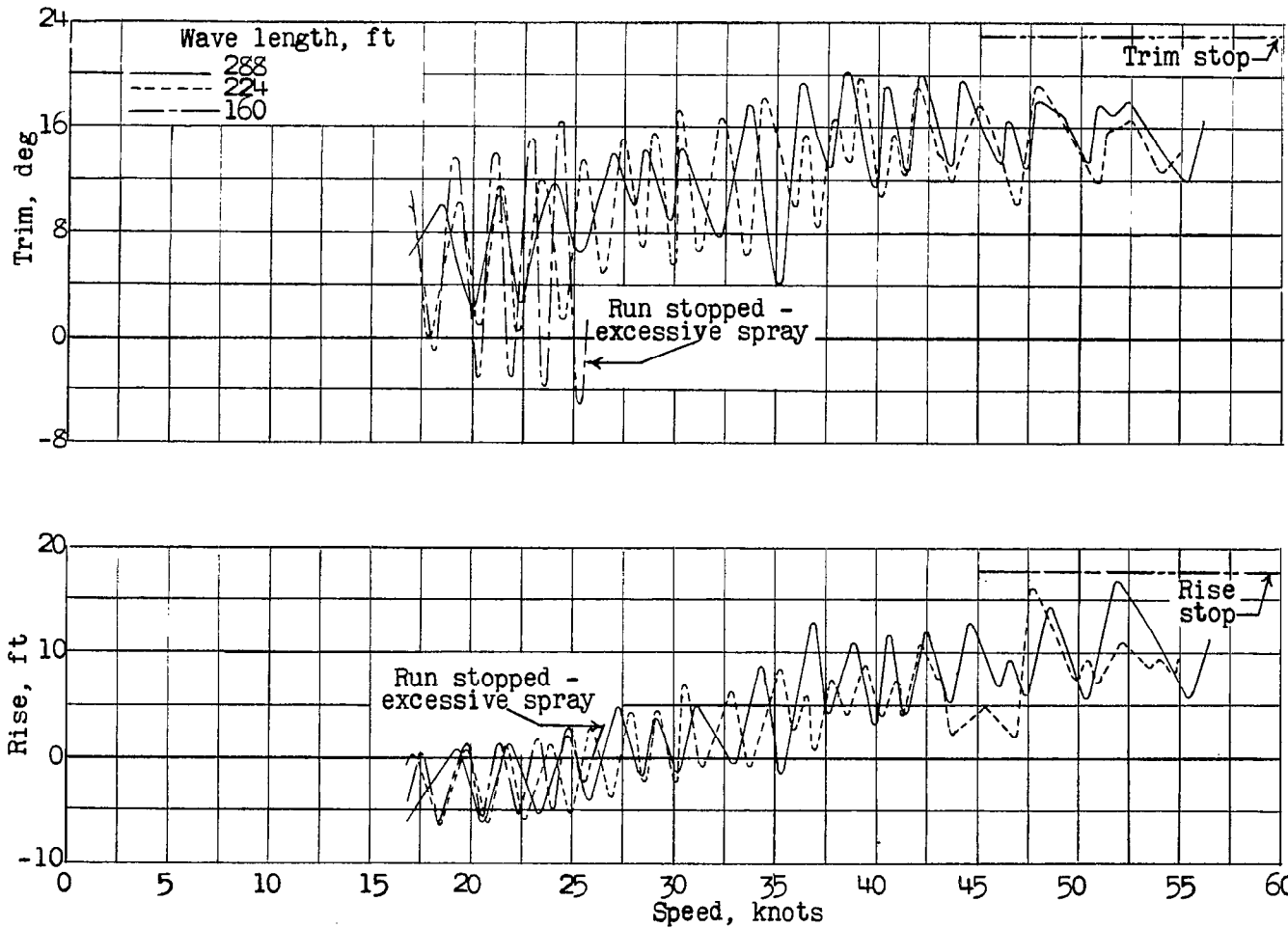
(a) Waves, 288 feet long.

Figure 29.- Aft-ski configuration (long strut); variation in trim and rise with elevator deflection during take-offs in waves 6 feet high and of various lengths. Take-off power.



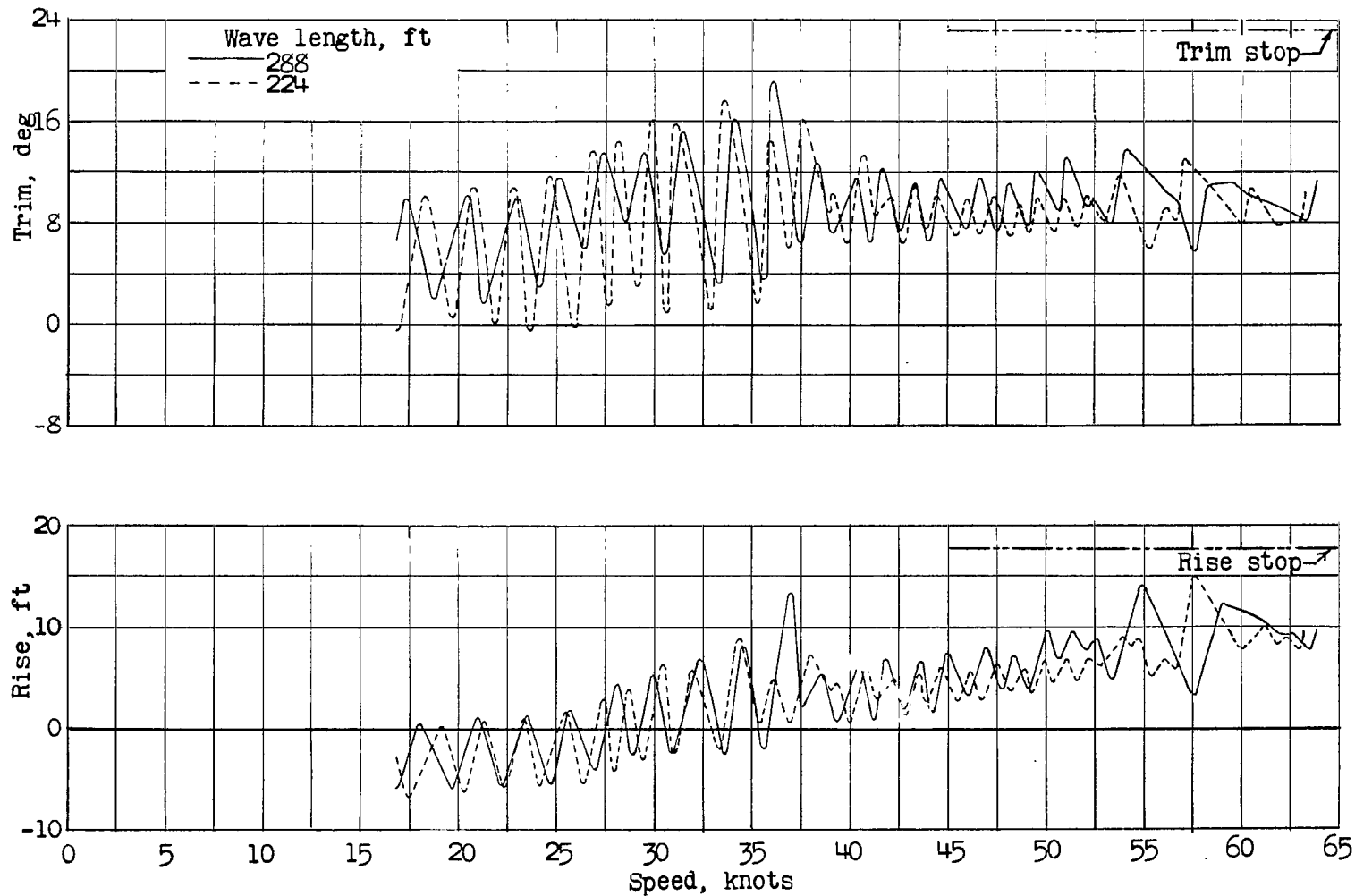
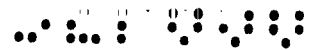
(b) Waves, 224 feet long.

Figure 29.- Concluded.



(a) Elevator deflection,  $-20^{\circ}$ .

Figure 30.- Aft-ski configuration (long strut); variation in trim and rise during take-offs in waves 6 feet high and various lengths. Take-off power.



(b) Elevator deflection,  $-10^{\circ}$ .

Figure 30.- Concluded.

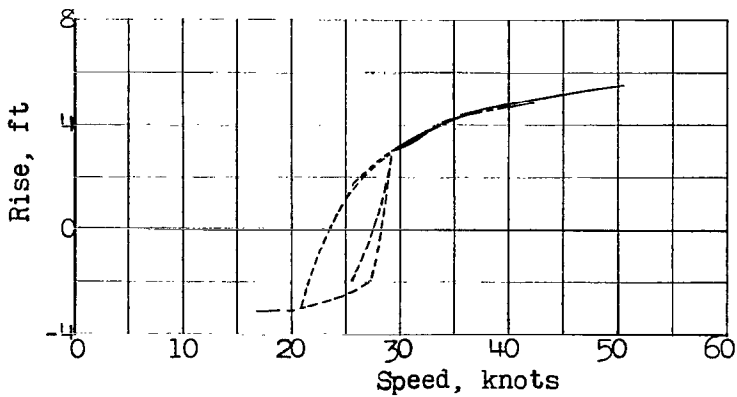
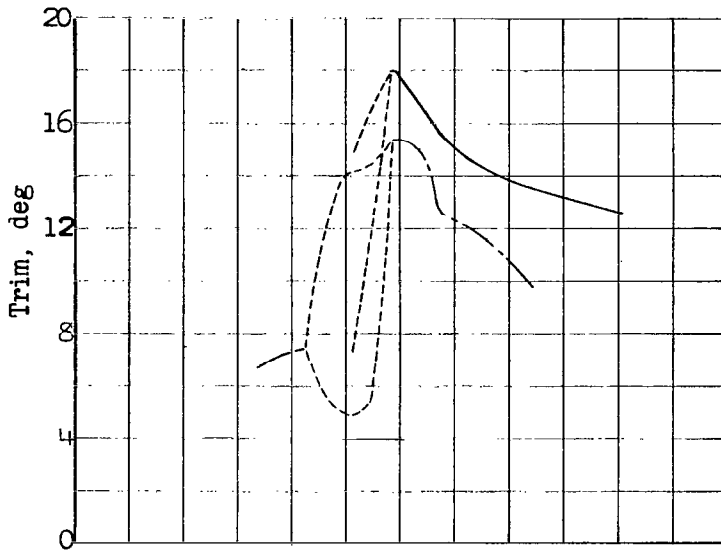
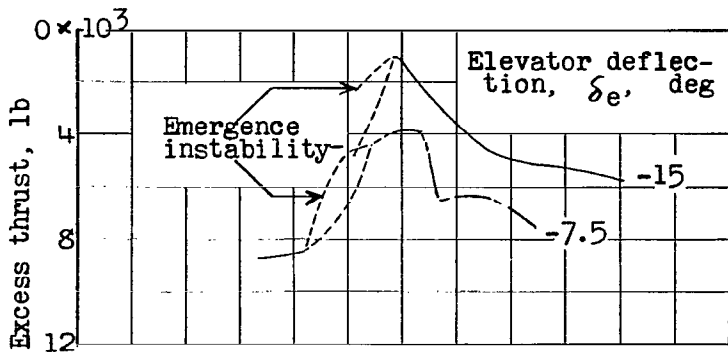


Figure 31.-  $2^\circ$  incidence, long-strut configuration; variation of excess thrust, trim, and rise with speed. Take-off power.

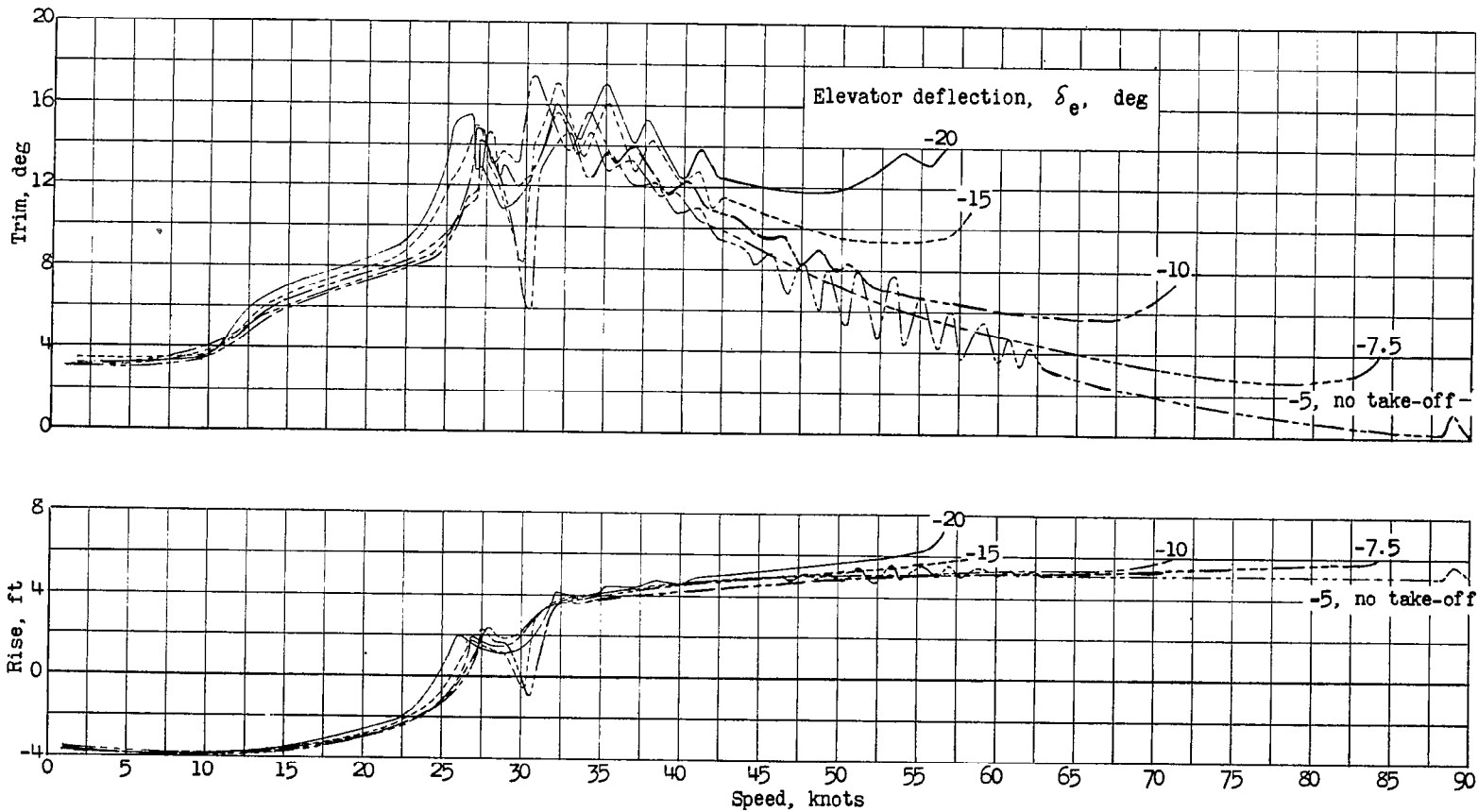


Figure 32.-  $2^\circ$  incidence, long-strut configuration; variation in trim and rise during take-offs in smooth water. Take-off power.

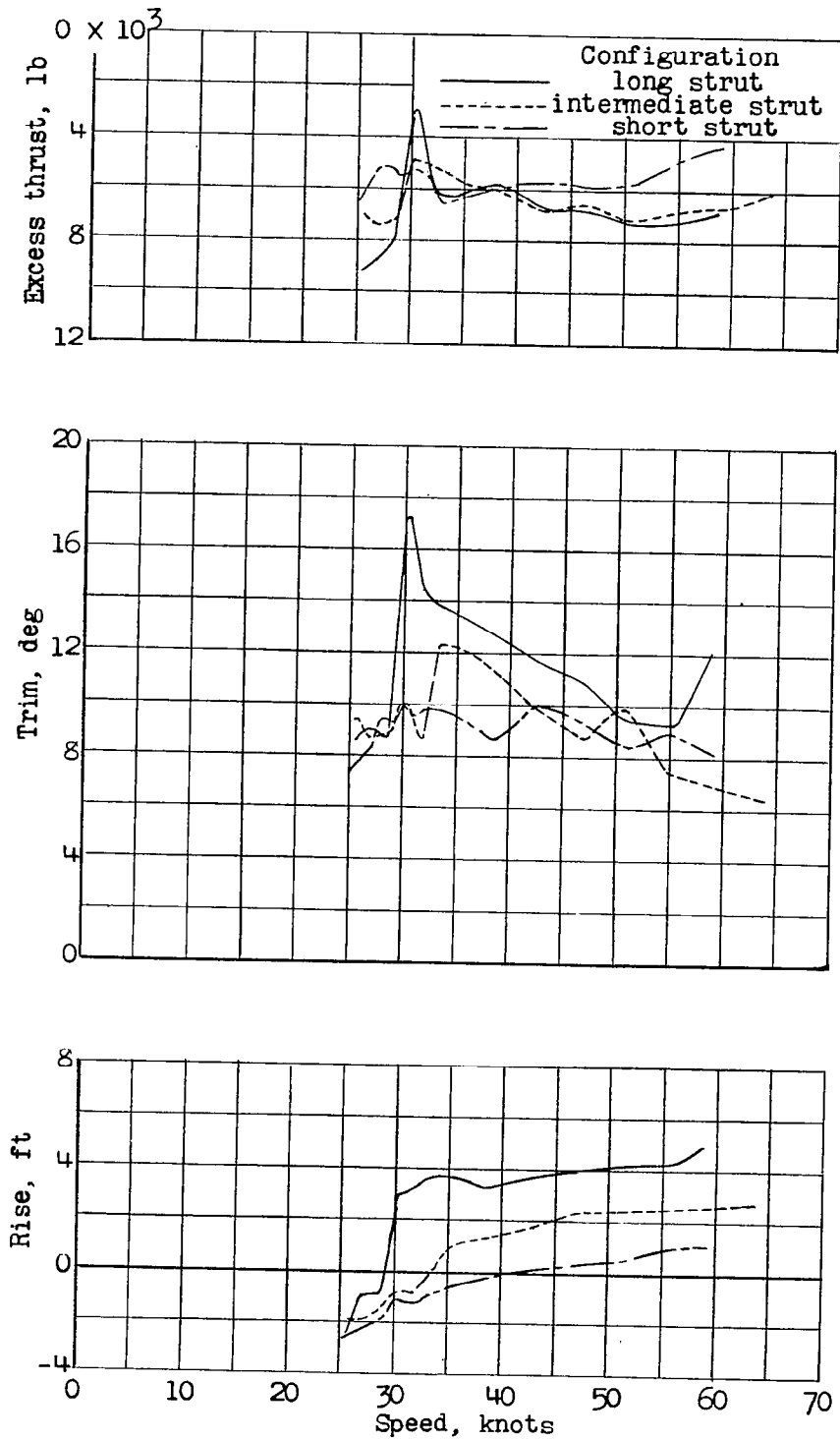


Figure 33.- Effect of vertical ski position on excess thrust, trim, and rise. Take-off power.

~~CONFIDENTIAL~~

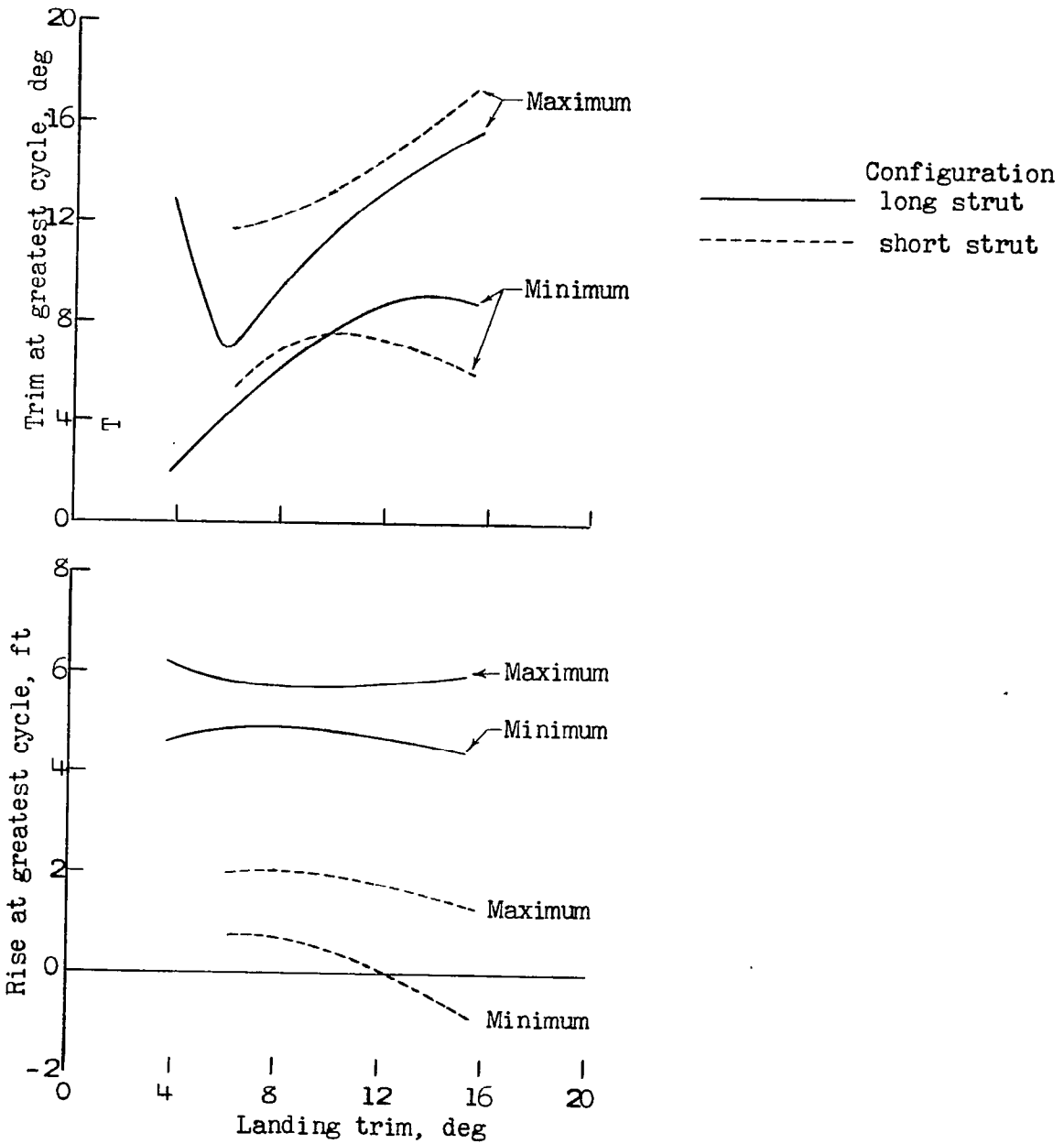


Figure 34.- Effect of strut length on trim and rise during smooth-water landing. Power-off.

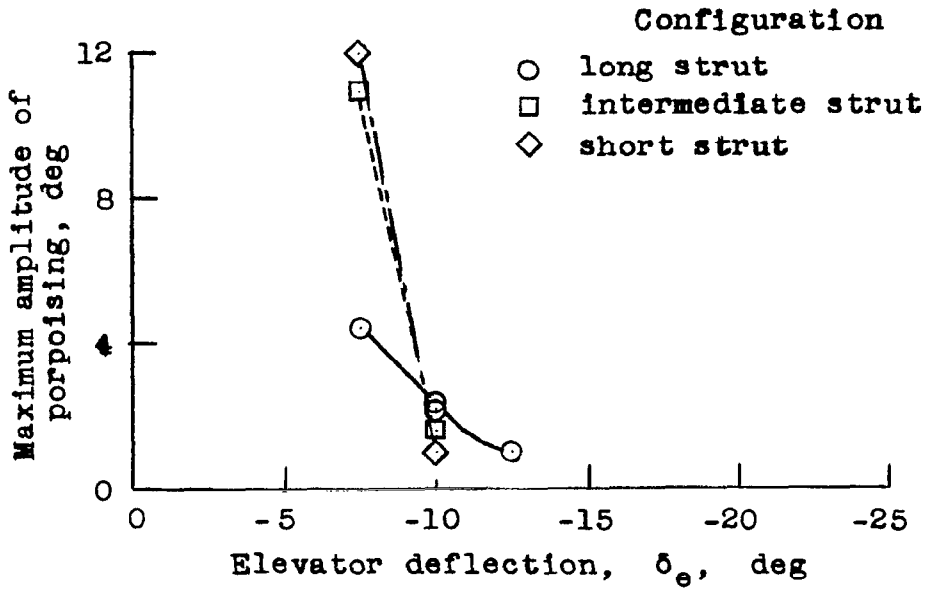


Figure 35.- Effect of strut length on the smooth-water take-off stability. Take-off power.

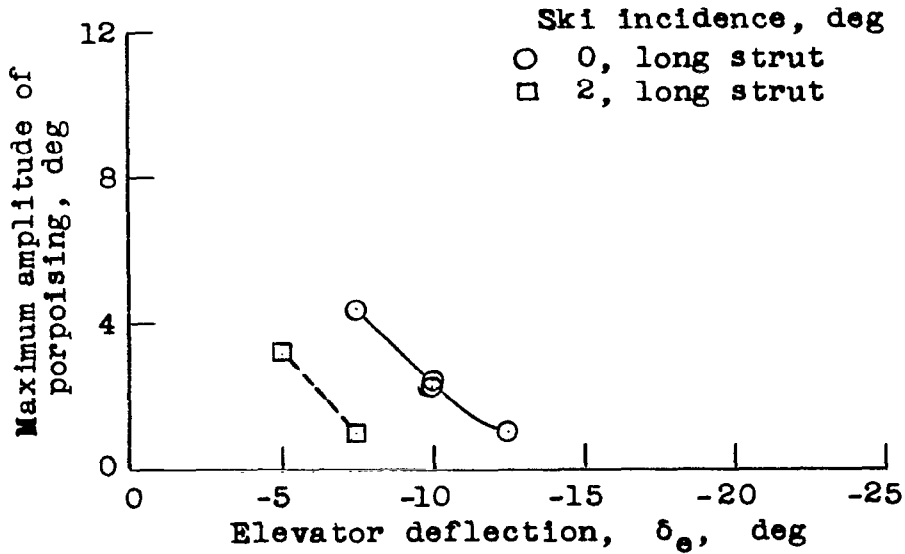


Figure 36.- Effect of ski incidence on the smooth-water take-off stability. Basic-ski configuration; take-off power.

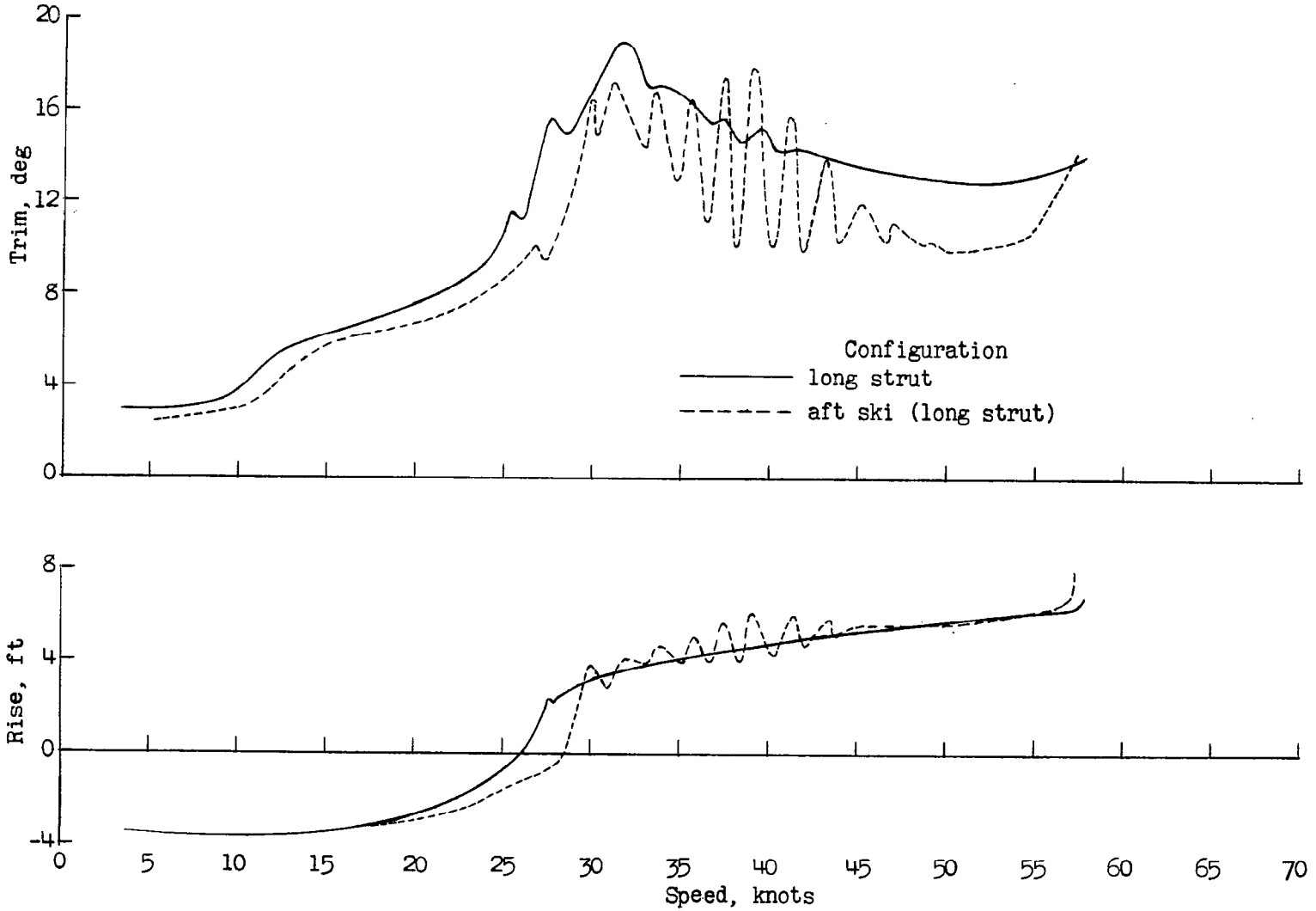


Figure 37.- Effect of longitudinal ski position on trim and rise during take-offs in smooth water.  $\delta_e = -20^\circ$ ; take-off power.

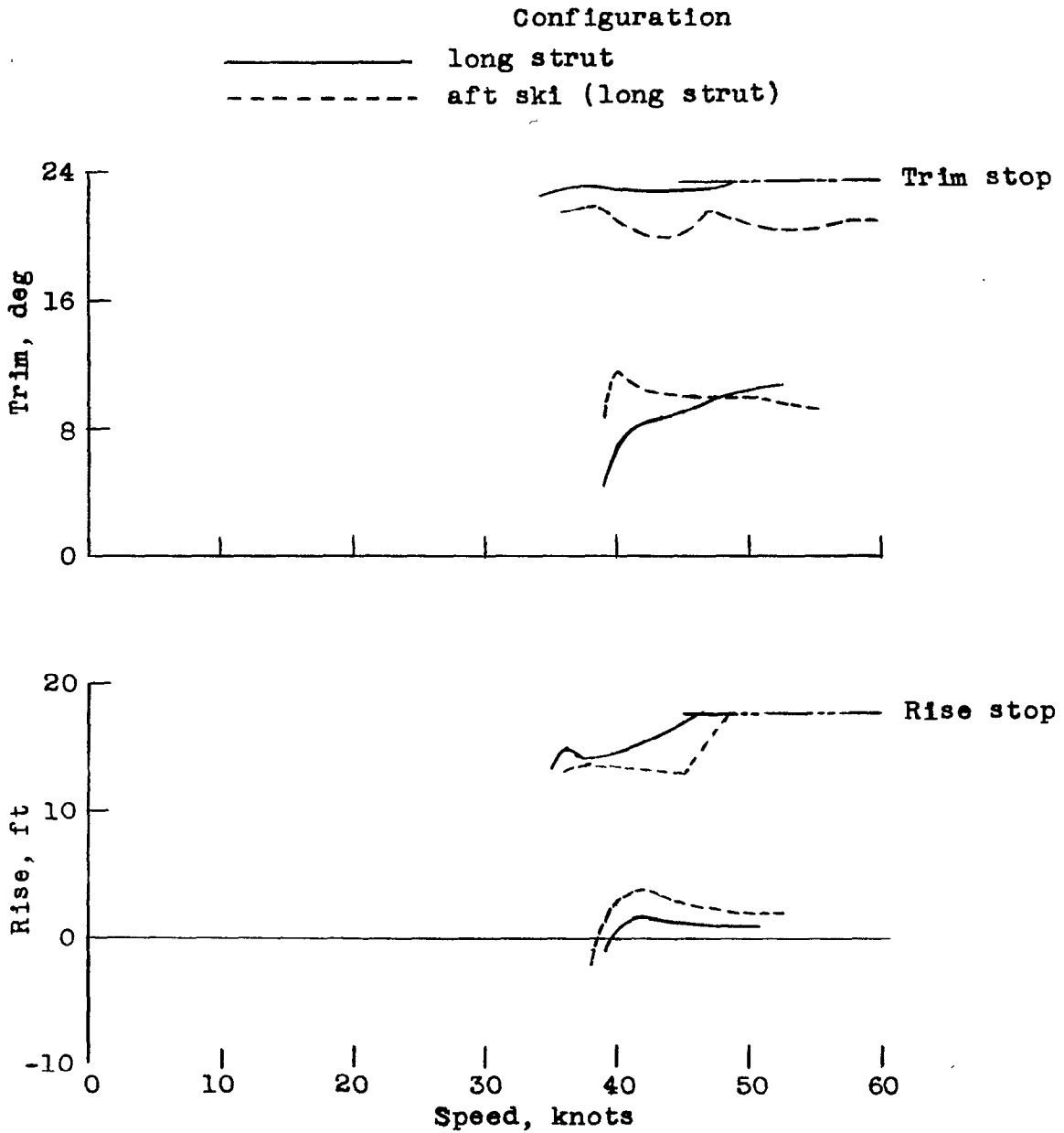


Figure 38.- Effect of longitudinal ski position on variations in trim and rise during take-offs in waves 6 feet high and 288 feet long.  $\delta_e = -20^\circ$ ; take-off power.

NASA Technical Library



3 1176 01438 6388

L

**CONFIDENTIAL**